



ELSEVIER

Contents lists available at ScienceDirect

## Journal of Hydrology: Regional Studies

journal homepage: [www.elsevier.com/locate/ejrh](http://www.elsevier.com/locate/ejrh)

# Geochemical evolution and mechanisms controlling groundwater chemistry in the transboundary Komadugu–Yobe Basin, Lake Chad region: An integrated approach of chemometric analysis and geochemical modeling

Abdulrahman Shuaibu<sup>a,b,\*</sup>, Robert M. Kalin<sup>a</sup>, Vernon Phoenix<sup>a</sup>, Ibrahim Mohammed Lawal<sup>a,c</sup>

<sup>a</sup> Department of Civil and Environmental Engineering, University of Strathclyde, Glasgow G1 1XJ, UK

<sup>b</sup> Department of Water Resources and Environmental Engineering, Ahmadu Bello University, Zaria 810107, Nigeria

<sup>c</sup> Department of Civil Engineering, Abubakar Tafawa Balewa University, Bauchi 740272, Nigeria

## ARTICLE INFO

## Keywords:

Groundwater quality  
Multivariate statistical analysis  
Geochemical modeling  
Hydrogeochemical characteristics  
Anthropogenic process

## ABSTRACT

**Study region:** The study is conducted in the transboundary Komadugu–Yobe Basin, Lake Chad region, a critical groundwater resource shared across national boundaries of Nigeria and Niger Republic.

**Study focus:** The research investigates geochemical evolution and sources of chemical constituents in groundwater through an integrated methodology that integrates geochemical modeling, molar ratios, bivariate plots, and chemometric analysis. Groundwater samples ( $n = 240$ ) were collected during wet and dry seasons to identify seasonal variations and the impact of geogenic and anthropogenic processes on groundwater quality.

**New hydrological insights:** The findings revealed that  $\text{Cl}^-$  and  $\text{NO}_3^-$  are associated with anthropogenic pollution. The Principal Component Analysis identified three main components associated with geogenic and anthropogenic processes, agricultural pollution, and mineral weathering. Hierarchical Cluster Analysis highlighted geogenic, anthropogenic, and evaporative influences. Groundwater in the basin is predominantly of  $\text{Ca-HCO}_3$  and  $\text{Na-Cl}$  types and is significantly undersaturated with calcite, dolomite, and fluorite, though seasonal variations show saturation in some samples. Elevated partial pressures of  $\text{CO}_2$  ( $p\text{CO}_2$ ) above atmospheric  $p\text{CO}_2$  in nearly all samples suggests active biogeochemical processes. Moreover, Gibbs plots, molar ratios, and bivariate plots, along with chloroalkaline indices (CAI-I & CAI-II) confirms influence of mineral weathering and ion exchange reactions within the aquifer system. Few locations show evaporation during the dry season. This study provides valuable insights for sustainable management of groundwater resources in semi-arid and arid regions.

## 1. Introduction

Geochemical modeling and chemometric analysis of groundwater quality is paramount for groundwater sustainability. The

\* Corresponding author at: Department of Civil and Environmental Engineering, University of Strathclyde, Glasgow G11XJ, UK  
E-mail address: [abdulrahman.shuaibu@strath.ac.uk](mailto:abdulrahman.shuaibu@strath.ac.uk) (A. Shuaibu).

<https://doi.org/10.1016/j.ejrh.2024.102098>

Received 26 September 2024; Received in revised form 25 November 2024; Accepted 27 November 2024

2214-5818/© 2024 The Author(s). Published by Elsevier B.V. This is an open access article under the CC BY license (<http://creativecommons.org/licenses/by/4.0/>).

demand for potable freshwater has significantly increased worldwide due to population growth, intensive agriculture, and pollution of surface and groundwater from both geogenic and anthropogenic activities (Awaleh et al., 2024; Elumalai et al., 2020; Mohammed et al., 2022; Samtio et al., 2023; Sikakwe and Eyong, 2022; Yang et al., 2021; Zhang et al., 2020). Groundwater provides drinking water supply for over one-third of the world's population (Ismail et al., 2020; Sheng et al., 2022). As a result, groundwater is overexploited globally, exposing it to significant risk of pollution and quality/quantity degradation (Elumalai et al., 2022; Ha et al., 2022; Mohammed et al., 2023; Sarti et al., 2021; Sheng et al., 2022; Yang et al., 2021). Consequently, groundwater quality is impacted by both natural and anthropogenic processes (Jabbo et al., 2022; Mohammed et al., 2023; Samtio et al., 2023; Subba Rao and Chaudhary, 2019) including factors such as leachate from dump sites, overexploitation of wells, accidental oil spillages, effluent from industries, residential wastewater, sewage, and intensive use of synthetic fertilizer (Awaleh et al., 2024; Shuaibu et al., 2024; Zhang et al., 2023). Natural processes that influence groundwater chemistry include rock–water reactions, oxidation–reduction, precipitation and dissolution of aquifer materials, and groundwater recharge and discharge processes (Elumalai et al., 2022; Jehan et al., 2019; Sikakwe and Eyong, 2022; Wali et al., 2019).

Groundwater is essential in arid and semi–arid regions (Elumalai et al., 2019; Loh et al., 2020; Mohammed et al., 2022). Aquifers in Komadugu–Yobe basin (KYB) are at risk of depletion and degradation due to overexploitation, climate change impacts, and pollution from geogenic and anthropogenic activities such as urbanization, industrialization, leachate from dumpsites, and indiscriminate discharge of solid wastes and wastewaters to the environment (Goni et al., 2019; Jagaba et al., 2020; Wali et al., 2020). Groundwater overexploitation in this region for domestic and irrigation water supply makes the aquifers vulnerable to depletion and quality degradation. The primary occupation of the residents in KYB is agricultural, including rain–fed and irrigation farming, contributing significantly to the food requirements in Nigeria (Adeyeri et al., 2020; Ahmed et al., 2018; Descloitres et al., 2013). It is crucial to know if groundwater in the basin meets the necessary quality standards for various uses. Several studies have recently been conducted in Komadugu–Yobe basin to evaluate groundwater quality (Abubakar et al., 2018; Bura et al., 2018; Garba et al., 2018; Goni et al., 2023; Hamidu et al., 2017; Ibrahim et al., 2021; Jagaba et al., 2020; Shuaibu et al., 2024; Suleiman et al., 2022). In contrast, geochemical modeling and chemometric analysis of groundwater at the regional scale remain challenging and had not yet been thoroughly investigated in the basin.

Geochemical modelling and chemometric analysis were employed in various studies worldwide to determine geochemical evolution and mechanisms influencing groundwater chemistry (Banda et al., 2024; Ding et al., 2024; Elumalai et al., 2019; Ha et al., 2022; Mohamed et al., 2022; Sikakwe et al., 2020; Spellman et al., 2024; Wang et al., 2024; Yang et al., 2021; Zhang et al., 2023). Chemometric analysis involves investigation of various water quality variables in a large hydrochemical data set simultaneously, compared to the univariate method, which involves evaluation of each variable in hydrochemical data set individually/using graphical methods (Liu et al., 2020; Rezaei et al., 2020; Sikakwe et al., 2020). The most effective way to examine hydrogeochemical datasets is by categorizing them into geospatial clusters with similar characteristics using chemometric analysis (Liu et al., 2020). It facilitates understanding the origin of dissolved ions in aquifer systems (Abdelaziz et al., 2020; Asomaning et al., 2023; Gautam et al., 2022; Liu et al., 2023; Sarti et al., 2021; Ullah et al., 2022). Graphical methods for assessing hydrochemical data are enhanced by employing multivariate statistical analysis (Gautam et al., 2022; Sikakwe et al., 2020; Singh et al., 2017). PCA is useful in reduction of large datasets into components and in assessing the interrelationship between different hydrochemical characteristics of analyzed water samples to understand sources and extent of pollution (Jehan et al., 2019; Wali et al., 2019). HCA is useful in identifying groups with similar characteristics in hydrochemical datasets (Elumalai et al., 2019; Kumar et al., 2018; Zhou et al., 2024). Groundwater geochemistry is usually influenced by geogenic processes and anthropogenic activities. Various factors, including aquifer lithology, travel time of groundwater, geological formations, sewage, effluent, leachates, and agrochemical applications, makes geochemical characterization of groundwater complex (Liu et al., 2020). However, the chemical reactions between water and minerals, as well as nature and characteristics of water that recharges the aquifer influences the hydrochemical characteristics of groundwater (Chen et al., 2020; Elumalai et al., 2020; Gautam et al., 2022; Kalin, 1996; Singh et al., 2017). Therefore, the interaction between water and mineral components of aquifer defines the general geochemistry of groundwater, providing valuable information on rock–water interaction process (Bradai et al., 2022; Kalin and Long, 1993).

The transboundary Komadugu–Yobe basin, located in the Lake Chad region, is characterized by intensive rainfed and irrigated agriculture, along with various industrial and domestic activities. The main source of water supply in this region is groundwater. Consequently, its significant exploitation results in a wide range of regional environmental problems, including degradation of groundwater quality/quantity. Although several studies have investigated groundwater quality in the transboundary Komadugu–Yobe basin, there has been limited research using integrated geochemical modelling and chemometric analysis on a regional scale. Previous studies in the basin focused on localized assessments of groundwater contamination, overlooking broader hydrogeochemical processes and various groundwater contamination sources. Therefore, this study has uniquely applied a combination of geochemical modelling, bivariate plots, molar ratios, and chemometric analysis to understand both geogenic and anthropogenic influences on groundwater chemistry at a basin-wide scale. It offers new insights into the impact of mineral weathering, ion exchange, and pollution from domestic and agricultural activities on groundwater quality, providing a comprehensive understanding that is critical for sustainable groundwater management. A conceptual model for groundwater evolution and distribution of geochemical processes controlling groundwater chemistry in KYB was established. The findings from this study are expected to support stakeholders and decision–makers in developing new insights into regional-scale groundwater management strategies in transboundary Komadugu–Yobe basin and the wider Lake Chad region.

## 2. The study area

The study area is the transboundary Komadugu–Yobe basin, a sub-basin of greater Lake Chad basin (Fig. 1a). The basin covers approximately 150,000 km<sup>2</sup>. The topographic elevation of the basin varies from 294 m in Yobe to 1750 m in Jos. The Komadugu Gana and Komadugu Yobe river systems flow through Yobe river and drains into Lake Chad (Adeyeri et al., 2019; Gana et al., 2018). The Hadejia Nguru wetlands and its associated river systems support different economic activities such as agriculture, fish production, pastoralism, and trading to over 20 million people residing in the basin (Adeyeri et al., 2020; Ahmed et al., 2018). KYB has national and international value due to its various internationally shared water resources and wetlands, which boosts local, national, and international economies and requires transboundary integrated water resource management among several countries in the Lake Chad region (Adeyeri et al., 2020). The climate in the basin is arid to semi-arid, characterized by frequent droughts, significant rainfall variability, and intense evaporation (Adeyeri et al., 2019; Goes, 1999). The basin has an average annual temperature of 12 °C in December and January and 40 °C in the months of March and April. The basin has a relative humidity of about 40 % per year. A mean annual precipitation of 1360 mm is estimated in Jos, whereas an estimate of 400–600 mm were recorded in Nguru and Hadejia, occurring in April to September. Mean annual evapotranspiration rate of 203 mm/year was estimated in the basin (Adeyeri et al., 2017; Shuaibu et al., 2023). The basin is characterized by arable land, and the vegetation in the basin is dominated by a variety of shrubs, dense grasses, and grasslands with scattered trees (Adeyeri et al., 2019).

### 2.1. General geology and hydrogeology

Geologically, the basin mainly consists of Precambrian basement complex rocks, sedimentary quarternary formations and Jurassic younger granites (Fig. 1b). The Precambrian basement complex comprises crystalline rocks of Pan–African orogeny that have been

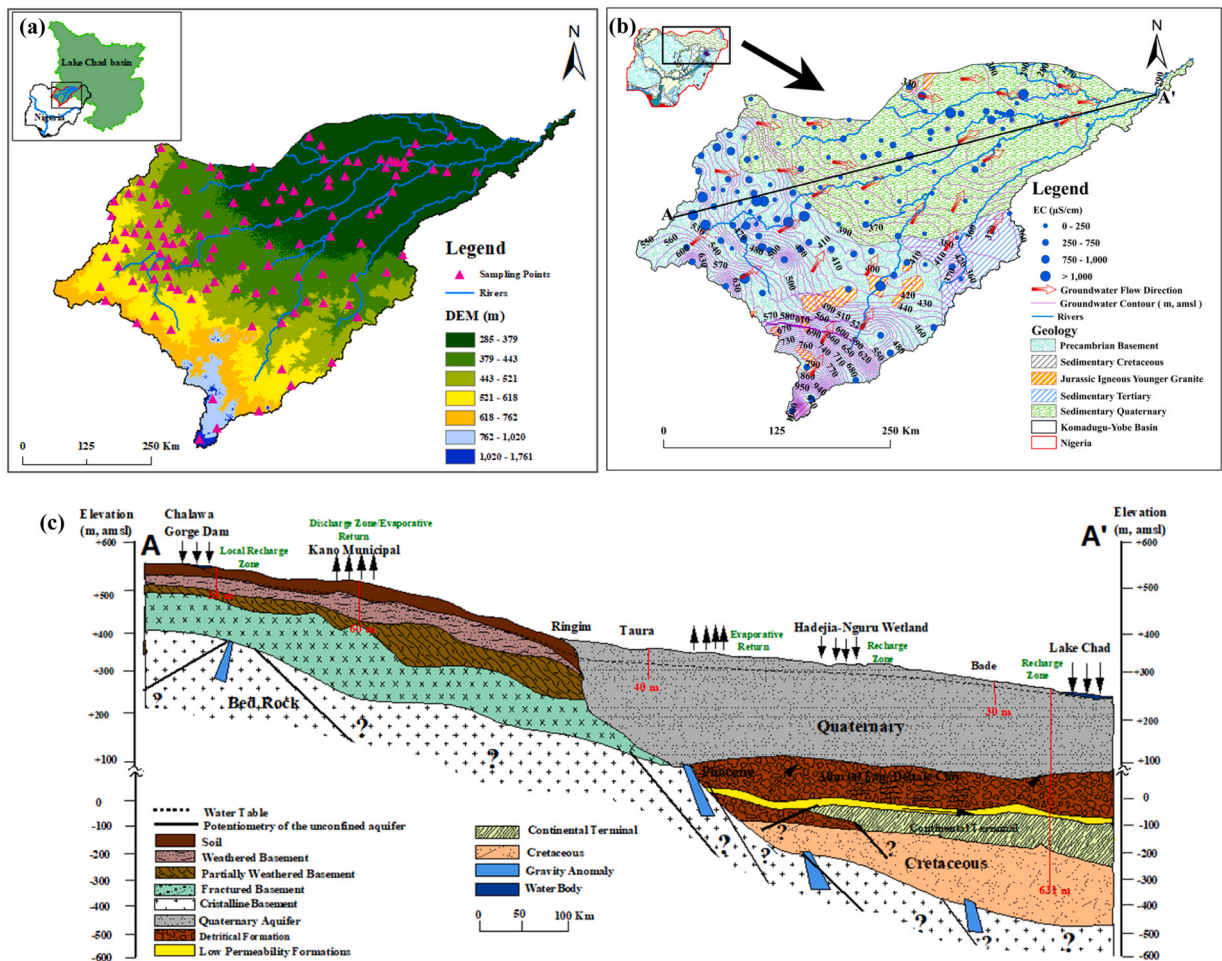


Fig. 1. (a) Study area map showing sampling locations, various Rivers and digital elevation model. The pink triangles represent groundwater sampling points (b) Generalised geological map showing groundwater flow direction and various geologic types (c) Hydrogeological cross-section A-A' of Komadugu–Yobe basin showing different lithologies, groundwater recharge and discharge zones and the groundwater table.

exposed and overlain by younger rocks (Schuster et al., 2009). These rocks consists of migmatite–gneiss, schists, and Pan–African granites that are mostly igneous and metamorphic rocks characterized by shallow weathered basement of low permeability. The mineral composition of the Precambrian basement complex are plagioclase, quartz, and biotite. The Precambrian basement is overlain by paleozoic to quaternary sediment deposits in the north-east (Fig. 1c). Jurassic younger granites comprises syenites, biotite granites, gabbros, ignimbrites, and rhyolites form ring dyke structures around Ningi, Dutse, Shira, Birnin–Kudu and Riruwai. The mineralogical composition of the younger granites are pyroxene, olivine, amphibole, quartz, biotite and plagioclase. The stratigraphical sequence of sediment accumulation overlying the basement complex is the Palaeozoic, lower Cretaceous, Middle Cretaceous, Continental Hamadien, upper Cretaceous, and Continental Terminal (Maduabuchi et al., 2006; Obaje et al., 2004). The sedimentary quaternary consists of a fine to coarse grained sand with an alternation of sandy Aeolian deposits. The valley consists of clayed to sandy fluvial sediments. The sedimentary basin pattern formed a complex subsurface deposit intercalated with sandy to clayey layers (Descloitres et al., 2013; Le Coz et al., 2011). The Chad formation has been continuously sedimented from the Late Miocene to the present, resulting in the deposition of Aeolian sand and clay elements (Shuaibu et al., 2022; Wali et al., 2020). Sand dunes and various alluvial deposits occurs in the Sedimentary Quaternary parts of the basin as a superficial deposits as parallel ridges extending several kilometers with a depth of 15–20 m which influence the river system around Kafin–Hausa, Miga, Jahun, and Auyo in the basin.

The primary source of groundwater in the basin is weathered basement, fracture basement and Plio–Pleistocene argillaceous sequence of Chad Formation with minor arenaceous horizons and recent Quaternary sediments (Fig. 1c). The basin has three distinct aquifer zones in the north-eastern parts: upper aquifer, middle aquifer, and lower aquifer (Goni, 2006). The upper and middle aquifer are accessible for exploitation. However, alluvial deposits on the river floodplains along Hadejia River and Hadejia–Nguru wetlands provides groundwater at shallow depth through tube wells (Tukur et al., 2018). The upper unconfined aquifer zone consists of quaternary deposits, including sands from the lake edge and alluvial fans /deltaic sediments of varied sizes. The aquifer comprises three distinct units: an upper A unit, which is below the water table, and two other units, namely the upper B and C units, ranging from semi–confined to confined (Bura et al., 2018; Goni, 2006). The thickness of the upper aquifer varies from 15 to 100 m with depth to water table of around 20 m. This aquifer is recharged through rainfall runoff and has a transmissivity varying from 0.6 to 8.3 m<sup>2</sup>/day (Maduabuchi et al., 2006). The middle aquifer is composed of sand beds 10–40 m thick interbedded with clay and diatomites, as well as sand fractions of moderately coarse to finer quartz, feldspar, mica, and iron oxides. The average transmissivity of the middle aquifer is about 360 m<sup>2</sup>/day whereas the lower aquifer has a transmissivity value ranging from 33 to 105 m<sup>2</sup>/day.

The Komadugu–Yobe River exhibits a seasonal flow pattern mainly between the months of June and December (Descloitres et al., 2013). Groundwater availability is dominant in the southern parts while the northeastern parts have some surface water resources. Groundwater flow is directed from southern parts of the basin to the northeastern parts towards the Lake Chad (Fig. 1b). The flow of groundwater in basement complex aquifer system is highly localized. Recharge likely occurs in the Southern part around Chalawa gorge dam while the discharge and evaporative return occurs around Kano towards Ringim. Moreover, recharge in the North-eastern parts is predominant around the Hadejia–Nguru wetlands through Komadugu–Yobe valley and Lake Chad region. Groundwater recharge is focused at wetlands and Komadugu–Yobe valley and through seepage from river channels and as infiltration of floodwater and runoff along the Yobe floodplain (Carter and Alkali, 1996; Le Coz et al., 2011; Maduabuchi et al., 2006).

### 3. Materials and methods

#### 3.1. Groundwater sampling and laboratory analysis

In this study, 240 groundwater samples were collected in 50 mL polyethylene bottles from 120 boreholes and hand-dug wells over two sampling campaigns in August and September 2021 (wet season) and March and April 2022 (dry season) in KYB. Wells were pumped for a minimum of 5 minutes before sampling at each location to ensure the collection of samples free from contamination by borehole pipes and stagnant water. Prior to sampling, each sample bottle was rinsed twice with groundwater from the respective well. Groundwater samples were then filtered through a 0.45 µm acetate cellulose syringe filter into two 50 mL polyethylene bottles: one bottle was acidified with 0.4 mL of nitric acid for cation analysis, while the other bottle, reserved for anion analysis, was left unacidified. Groundwater samples were sealed with watertight lids and kept below 4 °C in icebox coolers until laboratory analysis in Civil and Environmental Engineering Laboratory, University of Strathclyde, Glasgow, UK. Location of each sampled well were marked using a handheld portable global positioning system (GPS) and plotted on Fig. 1a. Prior to water samples collection, the pH, electrical conductivity (EC) were measured in-situ at each sampling location with hand-held digital electrical conductivity meter (Model 99720 pH/Conductivity meter). The equipment was calibrated using standard solutions before measurement. Total alkalinity was measured in-situ using a HACH digital alkalinity titrator (Model 16900, HACH International, Loveland, CO, USA). The major cations (Na<sup>+</sup>, K<sup>+</sup>, Ca<sup>2+</sup>, Mg<sup>2+</sup> and Fe) were analysed with inductively coupled plasma optical emission spectrometry (ICP–OES, iCAP 6200, Thermo Fisher Scientific), while analysis of the anions (Cl<sup>-</sup>, F<sup>-</sup>, SO<sub>4</sub><sup>2-</sup>, NO<sub>3</sub><sup>-</sup>) was achieved using ion chromatography instrument (Metrohm 850 Professional IC).

#### 3.2. Quality control and assurance

The quality of the fieldwork followed standard procedures to ensure the integrity of groundwater samples and in-situ measurements. The field equipment was calibrated before the start of field measurement using standard solutions and procedures. The preventive course of action and standard operating procedures (SOP) were adhered to in the field, throughout transportation, preservation, and in laboratory analysis to avoid sample aging and cross–contamination as recommended by APHA (2012). Laboratory



analysis accuracy and precision were confirmed by running standards and blanks. Finally, the reliability and accuracy of hydrochemical data were ensured by assessing ionic balance error, which was within the acceptable threshold of  $\pm 10\%$  with significant percentage of wet and dry season samples below  $\pm 5\%$ .

### 3.3. Multivariate statistical analysis (Chemometric methods)

Various hydrogeochemical studies conducted globally employed chemometric approaches, including correlation matrix analysis, PCA, and HCA (Kumar et al., 2018; Liu et al., 2023; Samtio et al., 2023; Singh et al., 2017; Subba Rao and Chaudhary, 2019; Ullah et al., 2022; Yang et al., 2021). These methodologies are employed to evaluate overall water quality by identifying pollution sources and to effectively disseminate water quality information (Rezaei et al., 2020). The Pearson's correlation analysis, PCA, and HCA were performed in this study using Origin Pro 2023b to determine the interrelationship of hydrochemical parameters and pollution source distribution of groundwater in Komadugu–Yobe basin.

#### 3.3.1. Pearson's correlation analysis

Pearson's correlation analysis was employed to classify groundwater quality variables and ascertain their interrelationships (Ullah et al., 2022). Pearson's correlation analysis was applied to identify anthropogenic activities and underlying rock properties that affect the groundwater chemistry. Major ions, such as nitrate, sulfate, sodium, and chloride, get into groundwater aquifers through municipal waste, the application of synthetic fertilizer in agricultural lands, and organic and inorganic wastes (Wali et al., 2019; Yang et al., 2021).

#### 3.3.2. Principal component analysis (PCA)

PCA was used to elucidate the relationship between large number of groundwater quality parameters (Kumar et al., 2018; Liu et al., 2023). It was applied in this study to identify potential sources of pollution, and statistical independent source tracers were chosen using Varimax rotation method with Kaiser normalization (Kumar et al., 2018; Yadav et al., 2020). The PCA was carried out on 13 groundwater quality variables, namely: pH, EC, TH,  $\text{Na}^+$ ,  $\text{K}^+$ ,  $\text{Ca}^{2+}$ ,  $\text{Mg}^{2+}$ ,  $\text{Cl}^-$ ,  $\text{HCO}_3^-$ ,  $\text{SO}_4^{2-}$ ,  $\text{NO}_3^-$ ,  $\text{F}^-$ , and Fe. The basic steps followed in the PCA are the standardization of data and extraction of principal components (PCs) (Wali et al., 2019). Principal components (PCs) with eigen value  $> 1$  were extracted from the scree plot. The variable in the respective components with higher loading were considered of greater significance regardless of sign. PCs are categorised into three classes: weak (0.30–0.50), moderate (0.50–0.750) and strong ( $> 0.75$ ) (Kumar et al., 2018).

#### 3.3.3. Hierarchical clustering analysis (HCA)

This study adopted HCA to classify the groundwater into groups that are similar to each other (Lima et al., 2019). Moreover, the study employed the R and Q-mode HCA using Ward's approach (minimal variance) to find the best clusters (groups) and for comprehensive result interpretation. Distance between samples were measured by squared Euclidean distance (Eq. (1)). Dendrograms are widely used to show hierarchical clustering or grouping together with the associated linkage distances (Subba Rao and Chaudhary, 2019). The cohesiveness and correlation between the hydrochemical parameters and groundwater samples were observed by constructing a dendrogram.

$$d_{xy} = \sum_{j=1}^p (x_j - y_j)^2 \quad (1)$$

where  $d_{xy}$  represents squared Euclidean distance between two points,  $x$  and  $y$ , in  $p$ -dimensional space.  $j$  is used to define each individual parameter (Kumar et al., 2018).

### 3.4. Geochemical modeling

Groundwater chemistry is mainly influenced by factors including structure and composition of mineral, and rock–water equilibrium (Elumalai et al., 2022; Kumar et al., 2018). Saturation index (SI) elucidates the equilibrium between water and minerals (Eq. (2)). The groundwater saturation indices for KYB were determined using Geochemist's WorkBench GWB software 17.0. SI value of zero shows that mineral saturation is in equilibrium in the aquifer, whereas positive value of SI signifies over-saturation of minerals in water and negative SI value signifies under-saturation of minerals in water.

$$SI = \log \left[ \frac{IAP}{K_{SP}} \right] \quad (2)$$

IAP represents the ion activity product in the solution, while  $K_{SP}$  represents the solubility product or equilibrium constant of the reaction.

### 3.5. Chloro-alkaline indices (CAI)

The chloroalkaline indices (Eqs. (3) and (4)) were used to study ion exchange reactions occurring within aquifers of the study area. These indices were used in various studies to better understand general groundwater chemistry, ion exchange mechanisms, and

rock–water interactions (Chen et al., 2020; Elumalai et al., 2022; Liu et al., 2023; Mohamed et al., 2022; Sikakwe and Eyong, 2022).

$$CAI - I = \frac{Cl^- - (Na^+ + K^+)}{Cl^-} \quad (3)$$

$$CAI - II = \frac{Cl^- - (Na^+ + K^+)}{SO_4^{2-} + HCO_3^- + CO_3^{2-} + NO_3^-} \quad (4)$$

Where all ions are measured in meq/L.

## 4. Results and discussion

### 4.1. Hydrochemical characteristics

The hydrochemical characteristics of the groundwater in KYB are presented in Table 1. The concentration of hydrochemical parameters in wet and dry seasons groundwater samples displayed a wide variation. pH values varied from 5.52 to 8.24 with a mean of 7.2 in wet season and those of dry season varies from 4.81 to 8.30 with a mean of 6.4 indicating acidic to weak alkaline water in respective seasons. EC ranges from 15 to 2746  $\mu\text{S}/\text{cm}$ , with an average of 462  $\mu\text{S}/\text{cm}$  and 54–3560  $\mu\text{S}/\text{cm}$ , with a mean of 538  $\mu\text{S}/\text{cm}$  in wet and dry season respectively. A significant number of samples in both season have EC values < 1500  $\mu\text{S}/\text{cm}$ , while some samples have EC value between 1500 to 3000  $\mu\text{S}/\text{cm}$  and a few of dry season samples have EC > 3000  $\mu\text{S}/\text{cm}$ . Therefore the groundwater in this region is largely fresh to brackish water in both seasons. The total hardness (TH) values of wet season samples varied from 0.8 to 704 mg/L as  $\text{CaCO}_3$ , with mean of 138 mg/L as  $\text{CaCO}_3$ . Most of the groundwater samples in both season appeared to be soft. However, few samples ranges from hard to very hard waters in respective seasons. The major ions dominance occurs in an order of  $\text{Ca}^{2+} > \text{Na}^+ > \text{K}^+ > \text{Mg}^{2+} > \text{Fe}$  and  $\text{HCO}_3^- > \text{Cl}^- > \text{NO}_3^- > \text{SO}_4^{2-} > \text{F}^-$  for cation and anion and  $\text{Ca}^{2+} > \text{Na}^+ > \text{Mg}^{2+} > \text{K}^+ > \text{Fe}$  and  $\text{NO}_3^- > \text{HCO}_3^- > \text{Cl}^- > \text{SO}_4^{2-} > \text{F}^-$  for cation and anion in wet and dry seasons respectively. This variation in concentration is likely due to various anthropogenic and geogenic processes taking place within the study area. The hydrogeochemical analysis suggests that the wet season groundwater is mainly characterized by  $\text{Ca}^{2+}$ ,  $\text{HCO}_3^-$  and  $\text{Na}^+$ ,  $\text{Cl}^-$  ions and those of dry season were dominantly characterized by  $\text{Ca}^{2+}$ ,  $\text{HCO}_3^-$  and  $\text{Na}^+$ ,  $\text{NO}_3^-$  ions. This resonates with the findings of Wang et al. (2024) that the main cation and anion in the groundwater of Hutuo River alluvial-pluvial fan in China were  $\text{Ca}^{2+}$  and  $\text{HCO}_3^-$ . Similarly, Samtio et al. (2023) identified  $\text{Ca}^{2+}$ ,  $\text{Na}^+$ ,  $\text{HCO}_3^-$  and  $\text{Cl}^-$  as the main ions in the groundwater of chachro sub-district in Pakistan. The dominance of these ions in the groundwater of the study area could possibly reflectes the influence of rock-water interaction and dissolution processes of plagioclase, amphibole, pyroxene, orthoclase and biotite rock minerals as well as contamination from irrigation return flows, synthetic fertilizers, potassium compost, domestic and industrial discharges, leachates and nitrification from pit latrines (Shuaibu et al., 2024; Subba Rao et al., 2022; Yu et al., 2024). It is worth noting that, the high nitrate concentrations shown in Table 1 during the wet and dry seasons were measured in open dug wells and boreholes, where significant pollution is attributed to agricultural activities and leachate from unimproved pit latrines, particularly in the downstream areas of the basin. This corroborates the findings of Goni et al. (2023) in parts of the Hadejia-Jama'are-Komadugu-Yobe Basin, where a high nitrate concentration of approximately 1003 mg/L was measured in a dug well affected by agricultural pollution.

### 4.2. Chemometric analysis

#### 4.2.1. Pearson's correlation analysis

Correlation analysis provides an understanding of the relationship between variables for assessing their communal origin and/or

**Table 1**

Descriptive statistics of hydrochemical parameters of wet and dry seasons groundwater.

Parameters	Range	Wet Season		Range	Dry Season	
		Mean	Std Dev.		Mean	Std Dev.
pH	5.52–8.24	7.2	0.6	4.81–8.30	6.41	0.5
EC	15–2746	462	470	54–3560	538	590
TH	0.8–704	138	125	5–1280	139	180
$\text{Na}^+$	2–285	36	45	1.8–247	33	40
$\text{K}^+$	0.1–96	10	20	0.7–173	9	20
$\text{Ca}^{2+}$	0.2–227	39	35	1.6–399	40	55
$\text{Mg}^{2+}$	0.9–58	9.9	10	0.2–69	9.2	10
$\text{Cl}^-$	0.7–372	48	70	1.6–645	58	90
$\text{HCO}_3^-$	1.5–379	120	85	0–220	64	45
$\text{SO}_4^{2-}$	0.1–133	15	20	0.1–226	16	30
$\text{NO}_3^-$	BDL–314	42	55	BDL–927	65	140
$\text{F}^-$	BDL–2.3	0.3	0.5	BDL–2.4	0.7	0.5
Fe	BDL–19	0.98	3.0	BDL–12	0.66	2.0

Note: All units are in mg/L except for dimensionless pH, TH in mg/L as  $\text{CaCO}_3$ , and EC in  $\mu\text{S}/\text{cm}$ . Std Dev.: Standard Deviation. BDL: Below Detection Limit.

sources (Singh et al., 2017; Wali et al., 2022). Fig. 2a and b presented the result of Pearson’s correlation analysis of the hydrochemical parameters of wet and dry seasons. EC strongly correlated with TH ( $r^2 = 0.82$ ),  $\text{Na}^+$  ( $r^2 = 0.81$ ),  $\text{Ca}^{2+}$  ( $r^2 = 0.81$ ),  $\text{Mg}^{2+}$  ( $r^2 = 0.73$ ),  $\text{Cl}^-$  ( $r^2 = 0.83$ ), and  $\text{SO}_4^{2-}$  ( $r^2 = 0.73$ ) and moderately correlated with  $\text{HCO}_3^-$  ( $r^2 = 0.61$ ) in wet season samples, whereas TH ( $r^2 = 0.70$ ),  $\text{Na}^+$  ( $r^2 = 0.72$ ),  $\text{Ca}^{2+}$  ( $r^2 = 0.71$ ),  $\text{Cl}^-$  ( $r^2 = 0.74$ ), and  $\text{Mg}^{2+}$  ( $r^2 = 0.60$ ),  $\text{SO}_4^{2-}$  ( $r^2 = 0.67$ ),  $\text{NO}_3^-$  ( $r^2 = 0.60$ ) correlates with EC in dry season groundwater samples (Table SM1 & 2, Fig. 2a &b). There was a weak correlation between EC and  $\text{K}^+$  ( $r^2 = 0.41$ ), and  $\text{NO}_3^-$  ( $r^2 = 0.37$ ) in wet season groundwaters, and  $\text{K}^+$  ( $r^2 = 0.47$ ) and  $\text{HCO}_3^-$  ( $r^2 = 0.29$ ) in the dry season groundwater samples (Table SM2). pH does not correlate with  $\text{K}^+$  ( $r^2 = -0.04$ ), and  $\text{NO}_3^-$  ( $r^2 = -0.12$ ), both of which show a very weak correlation between other variables in wet season (Table SM1). Fluoride shows moderate correlation with  $\text{HCO}_3^-$  and  $\text{SO}_4^{2-}$  and weak correlation with all other variables in the wet season, and Fe shows no correlation with all parameters in both seasons.  $\text{Cl}^-$  significantly correlates with all parameters in wet season except pH,  $\text{K}^+$ ,  $\text{NO}_3^-$ ,  $\text{F}^-$  and Fe. Unlike the wet season, it is positively correlated with all water quality parameters except pH,  $\text{HCO}_3^-$ ,  $\text{F}^-$ , and Fe, which implies anthropogenic sources.  $\text{NO}_3^-$  and  $\text{Cl}^-$  displayed strong positive correlation during dry season, suggesting they were derived from both human and animal waste possibly from heavy application of chemical fertilizers, sewage and industrial effluents (Beshir et al., 2024; Dasari et al., 2024; Khan et al., 2023; Memon et al., 2023). Again, nitrate displayed a significant positive correlation with all variables in dry season except  $\text{HCO}_3^-$ ,  $\text{F}^-$ , and Fe, contrary to the wet season where the association is very weak except for  $\text{F}^-$  and Fe which shows no association. This could be attributed to the intensive use of synthetic fertilizer in irrigated areas, specifically in Kano Irrigation Project (KIP), Hadejia Valley Project (HVP), and other irrigation projects along Hadejia-Nguru parts of the basin (Shuaibu et al., 2024). This is inline with the findings of Bijay-Singh and Craswell (2021) that fertilizer N consumption in East and South Asia has adversely contributes to nitrate pollution of groundwater and surface water bodies. The correlation between  $\text{Mg}^{2+}$  and  $\text{Ca}^{2+}$  ( $r^2 = 0.83$ , wet season, and  $r^2 = 0.89$ , dry season) is an indication that magnesium in the groundwater is derived from either dissolution of carbonate minerals or weathering of silicate minerals such as biotite, pyroxene and amphibole in the study area. Likewise,  $\text{SO}_4^{2-}$  and  $\text{Ca}^{2+}$  displayed a moderate and strong positive correlation in the wet and dry season, signifying a probable dissolution of evaporate in dry season.

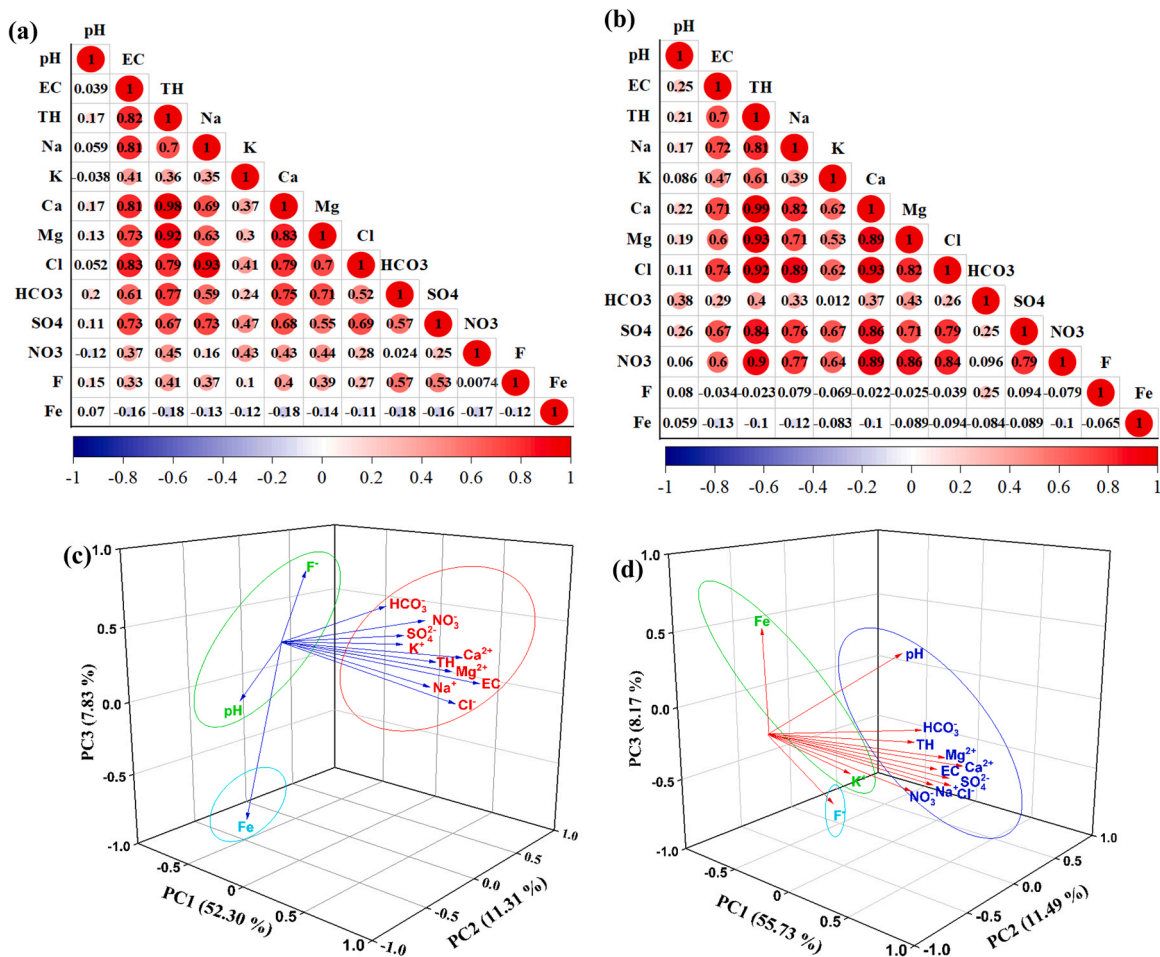


Fig. 2. . Pearson’s correlation analysis results (a) wet season (b) dry season. Loading plot of three PCs (PC1, PC2 and PC3) in 3D (c) wet season (d) dry season.

#### 4.2.2. Principal component analysis (PCA)

Principal Component Analysis (PCA) was conducted on 13 groundwater variables, namely pH, EC, TH, Na<sup>+</sup>, K<sup>+</sup>, Ca<sup>2+</sup>, Mg<sup>2+</sup>, Cl<sup>-</sup>, HCO<sub>3</sub><sup>-</sup>, SO<sub>4</sub><sup>2-</sup>, NO<sub>3</sub><sup>-</sup>, F<sup>-</sup>, and Fe in wet and dry season samples from the Komadugu–Yobe basin. This analysis aimed to understand the hydrogeochemical processes and identify sources of hydrochemical constituents within the groundwater of the basin. Three principal components (PCs) with eigenvalues greater than 1 were extracted for each season, as shown in Table 2. These components explain approximately 71.4 % and 75.4 % of the total variance for the wet and dry seasons, respectively. The loadings of the three PCs for the respective seasons are depicted in Figs. 2c and 2d, illustrating the relationship between variables. Notably, the first component exhibits a significant correlation among variables than the subsequent components in both seasons, indicating its primary influence on hydrochemical variations. In the wet season, the first principal component (PC1) accounts for 52.3 % of the variance in the groundwater dataset, with variables such as EC, TH, Na<sup>+</sup>, K<sup>+</sup>, Ca<sup>2+</sup>, Mg<sup>2+</sup>, Cl<sup>-</sup>, HCO<sub>3</sub><sup>-</sup>, and SO<sub>4</sub><sup>2-</sup> displaying substantial positive loadings (Table 2). This suggests that PC1 is heavily influenced by geogenic processes, including mineral weathering of minerals like plagioclase, biotite, amphibole, and orthoclase, as well as rock–water interactions. Additionally, anthropogenic contributions from domestic discharges and agricultural activities play a role in influencing groundwater chemistry. In this season, all variables exhibit positive loadings in PC1, except Fe, which shows a weak correlation with other variables. The second principal component (PC2), explaining 11.3 % of the variance, is marked by a strong negative loading on pH and significant positive loadings on K<sup>+</sup> and NO<sub>3</sub><sup>-</sup>. This pattern indicates non-point-source pollution from agricultural runoff and domestic waste. Elevated NO<sub>3</sub><sup>-</sup> levels likely result from nitrification processes associated with the intensive use of nitrogenous fertilizers and manure in rain-fed farming. Furthermore, the widespread use of unimproved pit latrines and septic tanks in recharge areas can lead to nitrate leachate in groundwater (Chen et al., 2024; Dasari et al., 2024; Nyambar and Mohan Viswanathan, 2024). The third principal component (PC3) in the wet season, explaining 7.8 % of the variance, has significant positive loading on F and Fe, likely reflecting the influence of mineral weathering and dissolution, coupled with variations in groundwater flow and sediment transport. These results corroborates with those obtained by Ait Said et al. (2023) in South-East of Morocco.

In the dry season, PC1 explains 55.7 % of the variance, with EC, TH, Na<sup>+</sup>, Ca<sup>2+</sup>, Mg<sup>2+</sup>, Cl<sup>-</sup>, SO<sub>4</sub><sup>2-</sup>, and NO<sub>3</sub><sup>-</sup> showing strong positive loadings. This component, like in the wet season, is influenced by mineral weathering and rock–water interactions, as well as anthropogenic inputs from agriculture and domestic sources (Bijay-Singh and Craswell, 2021; Dasari et al., 2024; Nyambar and Mohan Viswanathan, 2024). All variables, except F and Fe, exhibit positive loadings in PC1. The second component (PC2) in the dry season, accounting for 11.5 % of the variance, features significant loadings on pH, HCO<sub>3</sub><sup>-</sup>, and F, indicating a carbonate buffering effect that helps regulate groundwater pH. This buffering action suggests a distinct chemical environment compared to the wet season, with less contribution from agricultural runoff. Finally, PC3 in the dry season, which explains 8.2 % of the variance, again shows strong loading on F and notable loading on Fe. This component reflects the continued influence of mineral weathering and dissolution processes, particularly from biotite, pyroxene, and amphibole minerals (Dhaoui et al., 2023; Liu et al., 2023; Zhao et al., 2024).

#### 4.2.3. Hierarchical clustering analysis (HCA)

R–mode and Q–mode HCA were performed to 13 physicochemical parameters, to identify interrelationship between water quality parameters and samples with similar chemical composition using Ward’s method for wet and dry season samples. The R–mode HCA produces three cluster groups for both seasons (Fig. 3a and b, Table SM3). The first cluster reveals a strong correlation between EC, TH, Na<sup>+</sup>, Ca<sup>2+</sup>, Mg<sup>2+</sup>, Cl<sup>-</sup>, HCO<sub>3</sub><sup>-</sup>, SO<sub>4</sub><sup>2-</sup>, and F<sup>-</sup> for wet season samples. This suggests a mixed process of geogenic and anthropogenic inputs influence in the aquifer systems. Moreover, the dry season samples show an interrelationship between EC, TH, Na<sup>+</sup>, Ca<sup>2+</sup>, Mg<sup>2+</sup>, Cl<sup>-</sup>, SO<sub>4</sub><sup>2-</sup>, and NO<sub>3</sub><sup>-</sup> in the first cluster, suggesting geogenic processes of rock minerals and anthropogenic inputs (Dhaoui et al., 2023; Karmakar et al., 2023; Tziritis et al., 2024). However, cluster 2 in the respective seasons presented K<sup>+</sup> and NO<sub>3</sub><sup>-</sup>, and K<sup>+</sup>, implying influence of anthropogenic input from synthetic fertilizers and pit latrines leading to nitrification processes in the aquifer and a

**Table 2**

Component matrices of groundwater quality parameters, eigenvalues, % total variance and % cumulative total variance.

Parameters	Wet Season			Dry Season		
	PC1	PC2	PC3	PC1	PC2	PC3
pH	0.21	<b>-0.56</b>	-0.15	0.12	<b>0.74</b>	0.26
EC	<b>0.89</b>	0.16	0.04	<b>0.76</b>	0.20	-0.04
TH	<b>0.94</b>	0.06	0.12	<b>0.96</b>	0.19	-0.01
Na <sup>+</sup>	<b>0.86</b>	0.01	0.01	<b>0.84</b>	0.20	-0.12
K <sup>+</sup>	0.45	<b>0.51</b>	0.004	<b>0.71</b>	-0.17	0.06
Ca <sup>2+</sup>	<b>0.92</b>	0.06	0.12	<b>0.96</b>	0.17	-0.01
Mg <sup>2+</sup>	<b>0.86</b>	0.06	0.10	<b>0.88</b>	0.20	-0.02
Cl <sup>-</sup>	<b>0.89</b>	0.14	-0.07	<b>0.95</b>	0.06	-0.03
HCO <sub>3</sub> <sup>-</sup>	<b>0.76</b>	-0.33	0.32	0.22	<b>0.79</b>	-0.18
SO <sub>4</sub> <sup>2-</sup>	<b>0.80</b>	0.01	0.17	<b>0.87</b>	0.17	-0.03
NO <sub>3</sub> <sup>-</sup>	0.35	<b>0.72</b>	0.05	<b>0.94</b>	-0.09	-0.002
F <sup>-</sup>	<b>0.47</b>	-0.44	<b>0.45</b>	-0.11	<b>0.47</b>	<b>-0.53</b>
Fe	-0.06	-0.24	<b>-0.88</b>	-0.12	0.13	<b>0.83</b>
Eigenvalue	6.80	1.47	1.02	7.25	1.49	1.06
Total variance (%)	52.30	11.31	7.83	55.73	11.49	8.17
Cummulative total variance (%)	52.30	63.61	71.44	55.73	67.22	75.39



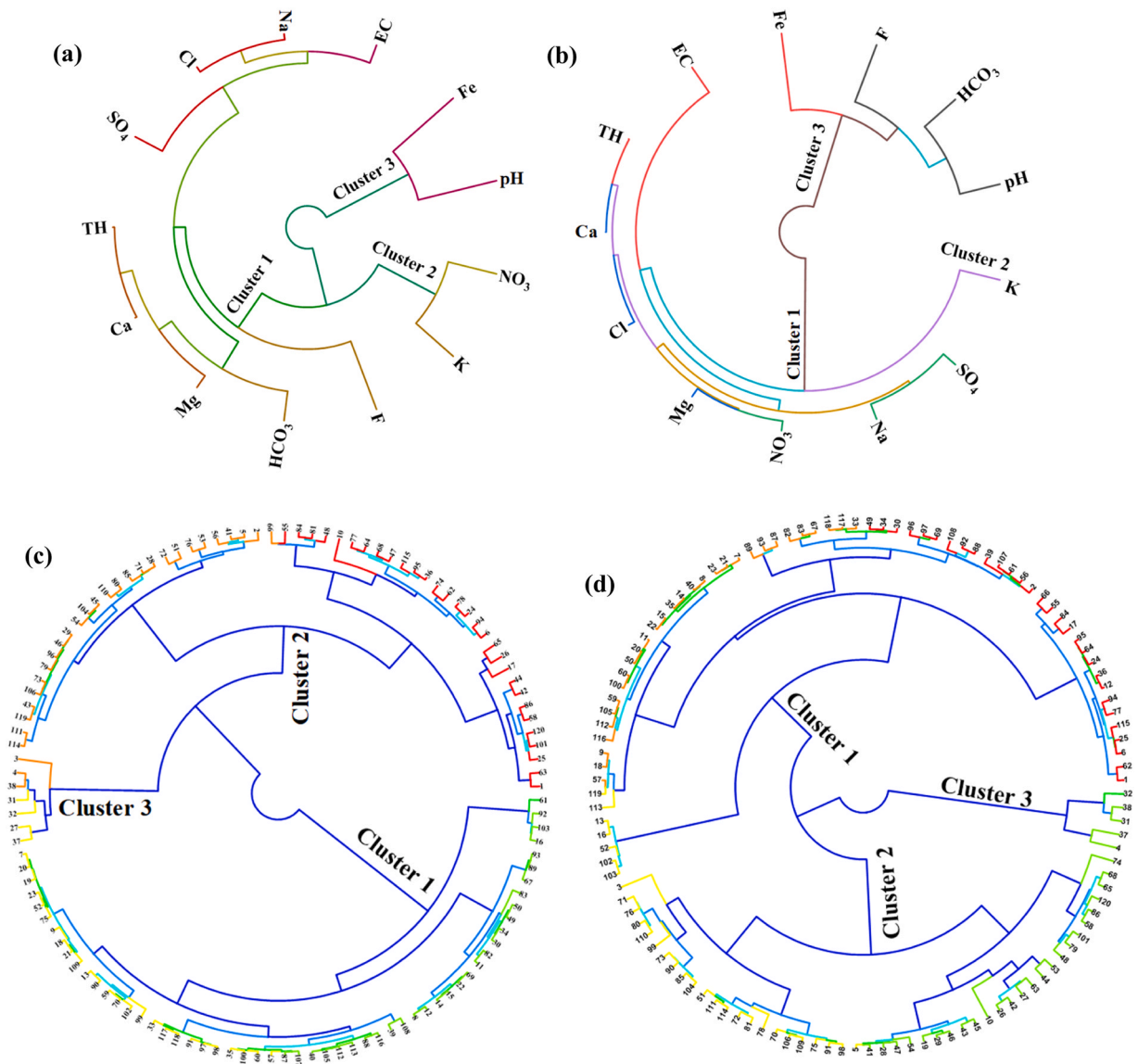


**Fig. 3.** Dendrogram of groundwater quality parameters showing different clusters (a) Wet season (b) Dry season. Dendrogram of sampling locations showing different clusters (c) Wet season (d) Dry season.

probable incongruent weathering of feldspar mineral (Bijay-Singh and Craswell, 2021). It is worth noting that cluster 3 is dominated by similar variables such as pH and Fe in wet season and pH, HCO<sub>3</sub><sup>-</sup>, F<sup>-</sup>, and Fe in dry season indicating slight variation in groundwater chemistry which could be due to interactions between various geochemical processes (Karmakar et al., 2023; Liu et al., 2020).

Like R-mode HCA, Q-mode HCA performed on groundwater sampling points produced 3 cluster groups in both seasons (Fig. 3c and d, Table SM4). The first cluster comprises 56 (46.7 %) groundwater samples for wet season and 67 (55.8 %) for dry season sampling points. The value of the EC in this cluster varies from 15 to 438  $\mu\text{S}/\text{cm}$  with mean of 175  $\mu\text{S}/\text{cm}$  and 54–1266  $\mu\text{S}/\text{cm}$  with mean of 324  $\mu\text{S}/\text{cm}$  in the respective seasons dataset, which indicates less mineralized water which is evident in the concentrations of all the groundwater quality parameters (Elumalai et al., 2022; Spellman et al., 2024; Tziritis et al., 2024). Cluster 2 contains 57 (47.5 %) and 48 (40 %) of the respective wet and dry seasons sampling points, with an EC range of 188–2746  $\mu\text{S}/\text{cm}$  with a mean value of 593  $\mu\text{S}/\text{cm}$  and 70–3560  $\mu\text{S}/\text{cm}$  with a mean value of 635  $\mu\text{S}/\text{cm}$ . This signifies moderately mineralized water influenced by anthropogenic inputs. Furthermore, cluster 3 accommodates fewer sampling points for both seasons, with only 7 (5.8 %) in wet season and 5 (4.2 %) in dry season. Groundwater in these sampling points have an EC value ranging from 960 to 2503  $\mu\text{S}/\text{cm}$  with mean value of 1732  $\mu\text{S}/\text{cm}$  and 1846 to 3320  $\mu\text{S}/\text{cm}$  with mean value of 2465  $\mu\text{S}/\text{cm}$ , signifying highly mineralized/low brackishwater influenced by geogenic (plagioclase, biotite and pyroxene weathering and dissolution), salinization sources, and evaporation processes (Elumalai et al., 2022; Tziritis et al., 2024). Fig. 4a and b presents the spatial distribution of groundwater cluster groups related to geology and electrical conductivities in the study area. It is obvious that the Precambrian basement parts of the basin were dominated by moderately and

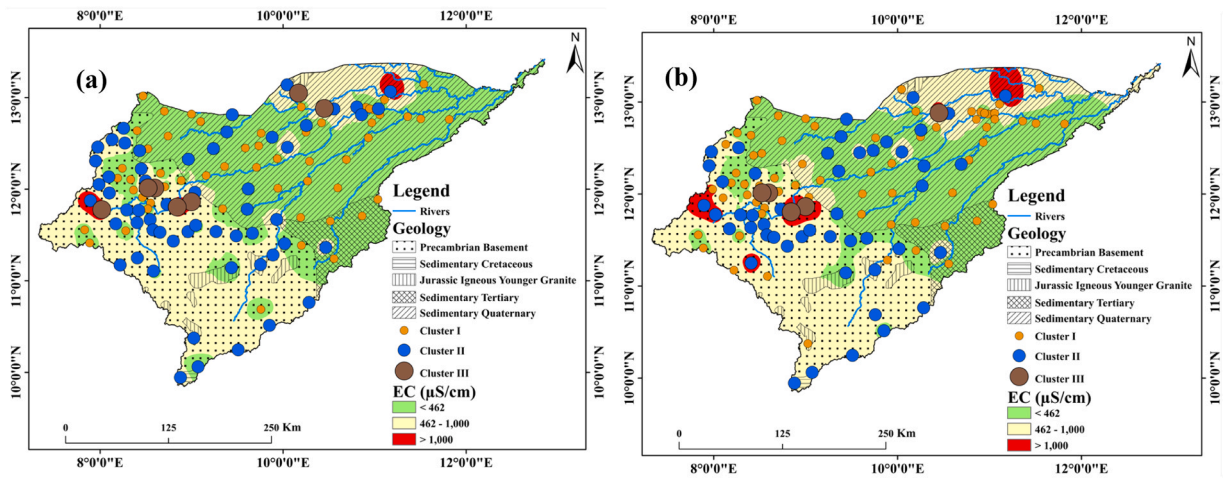


Fig. 4. Spatial distribution of groundwater clusters related with geology and electrical conductivities (a) wet season (b) dry season.

highly mineralized waters. This suggests weathering and dissolution of rock forming minerals (plagioclase, biotite, amphibole and pyroxine) in this region. However, less mineralized water predominates sedimentary quaternary parts of the study area.

### 4.3. Hydrochemical facies

The Piper (1944) diagram for hydrochemical classification is presented in Fig. 5a and b. Groundwater samples of wet season were plotted mainly in A, C, and D zones of lower-left triangle. This suggests the samples are characterized by sodium-type, calcium-type, and no dominant water type for cations. Moreover, the lower right triangle shows that groundwater samples of wet season were mainly plotted in G and F zones, signifying bicarbonate and chloride dominance. It is very clear that no samples are scattered in zones B and E, suggesting that  $Mg^{2+}$  and  $SO_4^{2-}$  are not among the major ions in wet season groundwater samples. Groundwater samples of wet season were projected onto zones 1, 2, and 4 of the central diamond-shaped plot (Fig. 5a). This suggests that wet season groundwater samples are mainly Ca -  $HCO_3$ , Na - Cl, and mixed water types. In the same vein, the dry season groundwater samples were plotted in D and C zones of lower-left triangle, and a few plotted in zone A, indicating  $Na^+$  and  $Ca^{2+}$  as the predominant cations in dry season groundwater samples (Fig. 5b). Furthermore, significant percentage of groundwater samples for dry season were plotted in G and F zones of lower-right triangle (Fig. 5b) indicating the presence of  $HCO_3^{2-}$  and  $Cl^-$  anions (Hu et al., 2024; Yang et al., 2024; Zhang et al., 2024). It is obvious that dry season samples exhibited a wide range of hydrochemical compositions, and the vast majority of the samples were scattered in 1, 3, and 2 zones of central diamond-shaped plot (Fig. 5b). This indicates that dry season groundwater samples were predominantly Ca - Na -  $HCO_3$ , Na - Cl, and mixed water types. In overall, groundwater of the study area in the

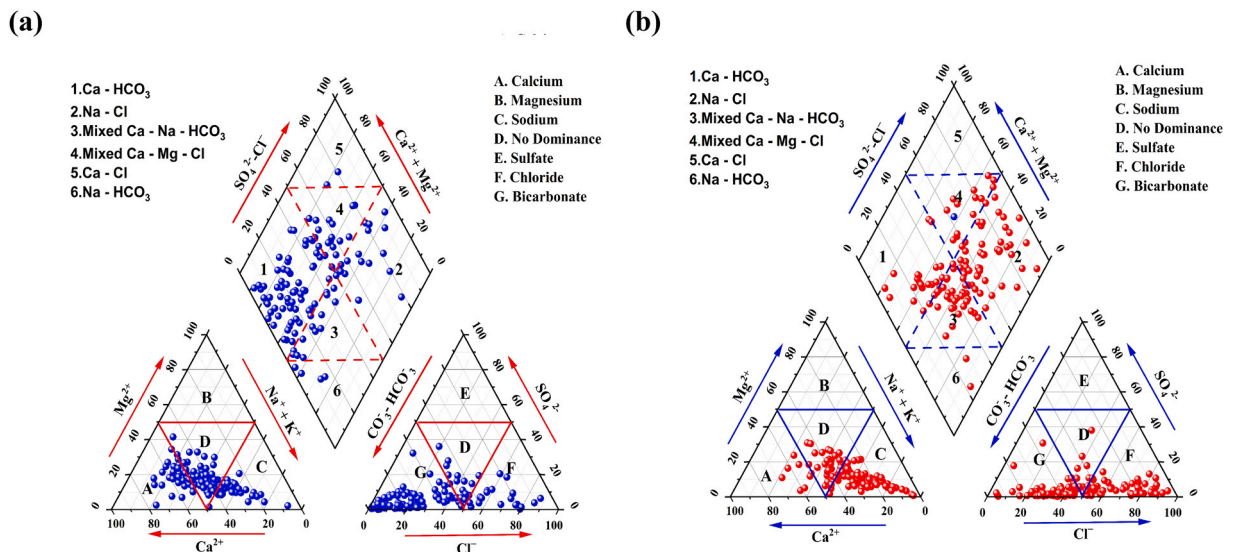


Fig. 5. Piper diagram for groundwater samples in Komadugu-Yobe basin (a) wet season (b) dry season.

respective seasons is greatly influenced by weathering of calcium and sodium feldspar minerals as well as anthropogenic contamination of surface water by irrigation return flows, drainage wastes and industrial discharges. Moreover, the dominance of Ca - HCO<sub>3</sub> water indicates dissolution of carbonates driven by soil CO<sub>2</sub> (Abu et al., 2024a and 2024b; Dasari et al., 2024; Elumalai et al., 2022; Liu et al., 2023; Subba Rao et al., 2022).

#### 4.4. Geochemical modelling

Geochemical modeling of aqueous solutions using Geochemist's WorkBench GWB software 17.0 was employed to ascertain rock–water–mineral interactions using groundwater quality datasets. These modeling techniques have been extensively used in assessing mineral weathering of silicate and carbonate minerals dissolution (Bradai et al., 2022; Elumalai et al., 2022; Ganyaglo et al., 2024; Liu et al., 2015; Trabelsi and Zouari, 2019).

##### 4.4.1. Saturation indices

In this study, Geochemist's WorkBench GWB software 17.0 was employed to determine saturation indices of various minerals in wet and dry seasons groundwater samples in Komadugu–Yobe basin (Table 3). It was observed that significant percentage of the samples shows undersaturation with respect to dolomite, calcite, and fluorite (Fig. 6) with some, 41 (34.2 %) and 4 (3.3 %), 27 (22.5 %) and 1 (0.83 %), and 1 (0.83 %) of the samples indicated near saturation with respect to dolomite, calcite, and fluorite in wet and dry seasons, respectively. Fig. 6 presents relationship between some selected saturation indices and electrical conductivities (EC). Few samples with high EC displayed over saturation with respect to dolomitic carbonate and calcite. It is noteworthy that dolomite saturation is a proxy indicating high magnesium ions in the groundwater samples. This could be due to incongruent weathering of feldspar minerals. Therefore, the occurrence of dolomite in the study area is highly unlikely. Calcite mineral may be the main source of high Ca<sup>2+</sup> and HCO<sub>3</sub><sup>-</sup> in the groundwater samples which results from congruent weathering and dissolution of calcite (Eq. (5)) (Elumalai et al., 2022; Ganyaglo et al., 2024). Moreover, carbonate minerals could be due to various rock minerals in the study area viz plagioclase, biotite, pyroxine and amphibole minerals. Fluorite saturation could be due to a common ion effect with carbonates together with weathering and dissolution of fluoride bearing minerals such as granite gneisses, fluorite and biotite minerals as a results of rock-water interaction under high alkaline condition which could be the main source of F<sup>-</sup> in the aquifers of the study area (Abu et al., 2024a and 2024b; Sunkari et al., 2025). Kumar et al. (2018) posit that fluoride concentration in aquifer system results from dissolution of biotite minerals (Eq. (6)). Fluoride concentration in groundwater could also results from dissolution of fluorite mineral (Eq. (7)).



Figs. SM1 and SM2 shows spatial distribution of saturation indices of groundwater samples related to geology and electrical conductivities (EC) for wet and dry seasons. The figures revealed that saturation indices above the mean values are largely concentrated in Precambrian basement parts of the study area. Furthermore, most of the oversaturation in both seasons for dolomite, calcite, and fluorite dominated in Precambrian basement complex region. This could be due to the presence of plagioclase, biotite, pyroxene and amphibole rock minerals in this region. However, few samples shows oversaturation with respect to dolomite, calcite, and fluorite in the sedimentary quaternary formation and sedimentary tertiary regions of the study area in the respective seasons.

##### 4.4.2. Partial pressures of carbon dioxide (pCO<sub>2</sub>)

Geochemical processes of groundwater and reaction between groundwater and carbonate minerals are greatly influenced by partial pressure of carbon dioxide (pCO<sub>2</sub>) which acts as a source of acid (H<sup>+</sup>) for mineral weathering reactions (Trabelsi and Zouari, 2019). The partial pressures of CO<sub>2</sub> of wet and dry season groundwater samples varied from 10<sup>-3.86</sup> to 10<sup>-1</sup> atm with a mean value of 10<sup>-2.36</sup> atm and 10<sup>-4.2</sup> to 10<sup>-1.34</sup> atm with an average value of 10<sup>-2.08</sup> atm, respectively. It was observed that about 96.7 % and 99.2 % of groundwater samples in wet and dry seasons have pCO<sub>2</sub> above atmospheric pCO<sub>2</sub>, which is about 10<sup>-3.5</sup> atm. This indicates the presence of CO<sub>2</sub> in the groundwater system due to biological activity such as respiration of vegetation roots and decomposition of soil organic matters. The partial pressure of CO<sub>2</sub> is observed to decrease as pH of wet and dry-season groundwater samples increases (Fig. SM3). This corresponds to the findings of (Adams et al., (2001); Elumalai et al., (2022); Liu et al., (2015) and Rajmohan et al., (2021)). Negative correlation of -0.61 and -0.21 were observed in groundwater samples of wet and dry seasons which might be

**Table 3**  
Descriptive statistics of mineral saturation indices.

Minerals	Wet Season				Dry Season			
	Min	Max	Mean	Std	Min	Max	Mean	Std
Calcite	-6.65	1.15	-0.88	1.24	-6.78	0.65	-2.17	1.31
Dolomite	-12.87	3.03	-1.27	2.52	-13.26	1.43	-3.85	2.66
Fluorite	-6.89	0.08	-2.64	1.38	-2.70	0.09	-1.43	0.53

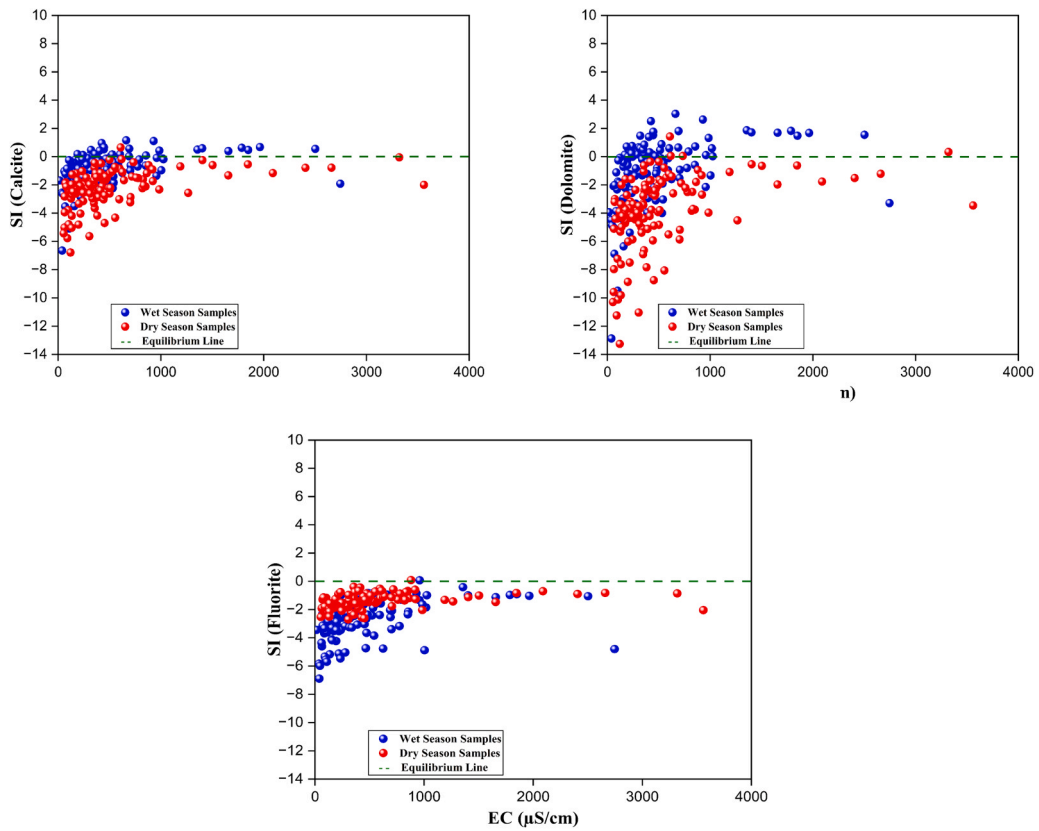
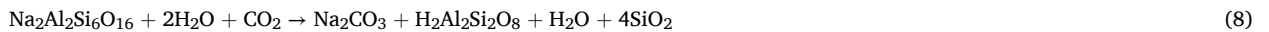


Fig. 6. Saturation indices of some selected minerals against electrical conductivity of groundwater samples of wet and dry seasons.

attributed to longer residence time, rock–water interaction in aquifer systems and biogenic activities that produces CO<sub>2</sub>. According to Liu et al. (2015), negative correlation between pCO<sub>2</sub> and pH signifies dissolution of feldspar along groundwater flow path, and following reaction could be possible in the aquifer formations (Eq. (8)):



This reaction resulted in the consumption of CO<sub>2</sub> and increase in concentration of Na<sup>+</sup> and HCO<sub>3</sub><sup>-</sup> leading to pH increase and partial pressure of CO<sub>2</sub> decrease. It is established that the decay of organic matter and roots respiration releases CO<sub>2</sub> which is the main source of HCO<sub>3</sub><sup>-</sup> in groundwater (Eqs. (9) and (10)).

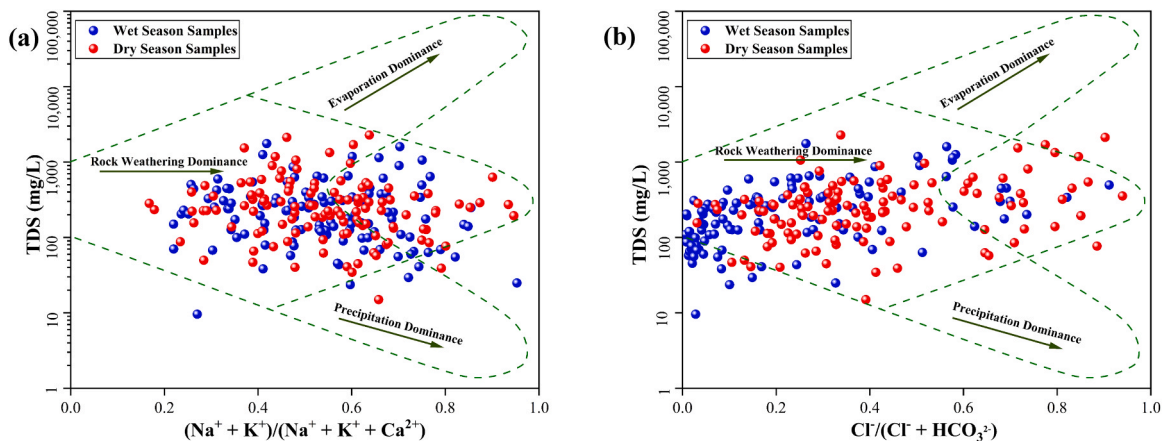
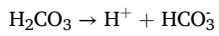


Fig. 7. Gibbs plots of geochemical processes governing groundwater chemistry (a) cations (b) anions.





(10)

4.5. Hydrogeochemical processes

Gibbs plots, molar ratios, and bivariate plots were employed in this study to estimate various hydrogeochemical processes that

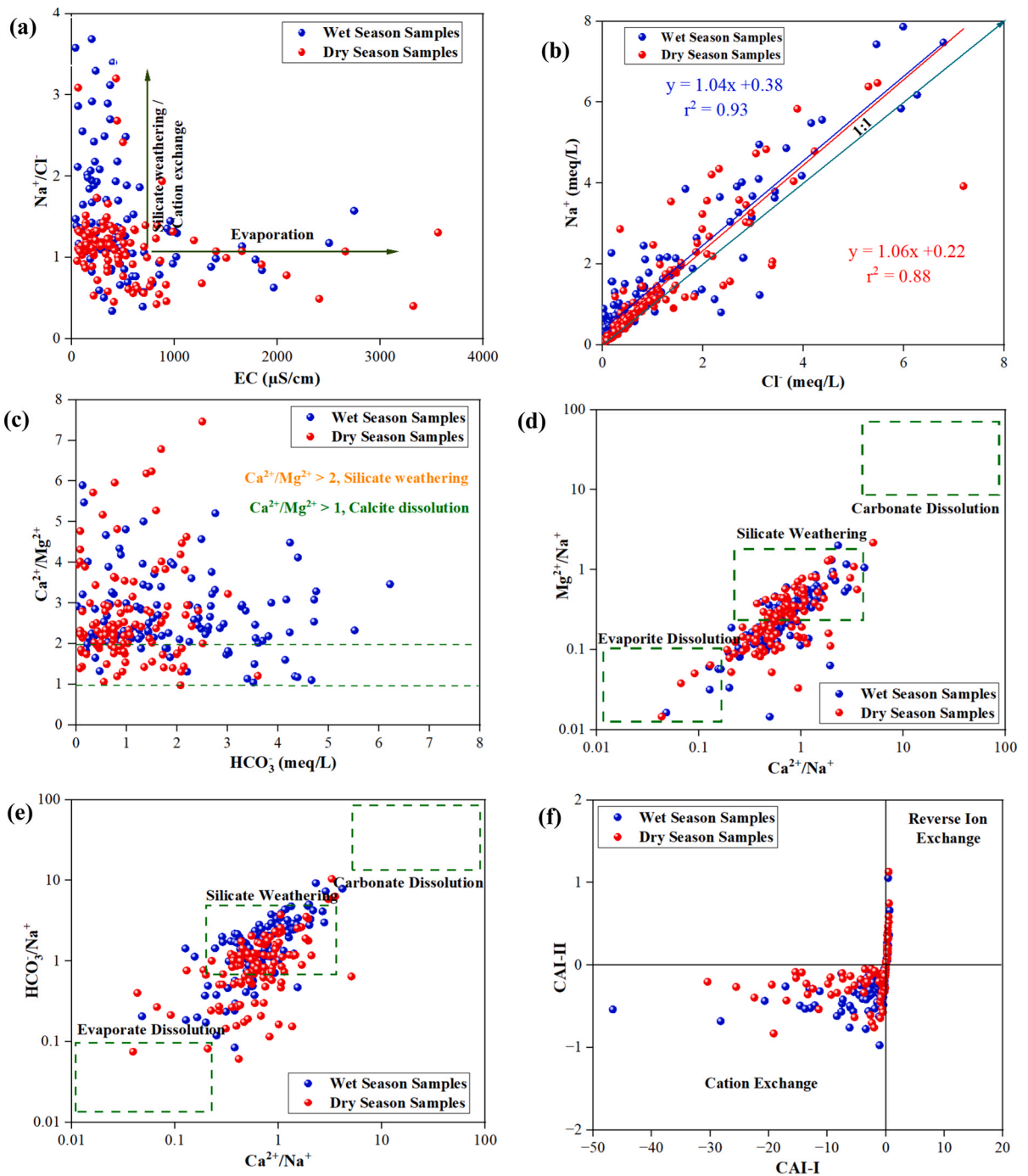


**Fig. 8.** Bivariate plots of: (a)  $\text{Na}^+/\text{Cl}^-$  vs. EC; (b)  $\text{Na}^+$  vs.  $\text{Cl}^-$  (c)  $\text{Ca}^{2+}/\text{Mg}^{2+}$  vs.  $\text{HCO}_3^-$  (d)  $\text{Mg}^{2+}/\text{Na}^+$  vs.  $\text{Ca}^{2+}/\text{Na}^+$  (e)  $\text{HCO}_3^-/\text{Na}^+$  vs.  $\text{Ca}^{2+}/\text{Na}^+$  (f) CAI-II vs. CAI-I.

influence groundwater chemistry in the study area.

#### 4.5.1. Gibbs plots

Gibbs plots (Gibbs, 1970) were used in this study to identify the major geochemical mechanisms influencing the groundwater chemistry of the study area (Fig. 7a and b). The figures show that majority of groundwater samples of wet and dry seasons were plotted in the region characterized by rock weathering/rock–water interaction dominance (Chen et al., 2024; Hu et al., 2024). A few samples with high TDS concentration during dry season were observed to trend towards evaporation dominance zone. Therefore, rock weathering is likely the predominant geochemical process controlling the chemistry of groundwater in the study area, except in a few areas associated with evaporation dominance during dry season.

#### 4.5.2. Evaporation

Evaporation process has potential to increase concentration level of all ions present in groundwater in semi– arid areas due to climate change impacts.  $\text{Na}^+/\text{Cl}^-$  vs EC plot was employed to determine influence of evaporation processes on chemistry of groundwater in the study area (Fig. 8a). According to Jankowski and Ian Acworth (1997), when evaporation has significant influence on the chemistry of groundwater,  $\text{Na}^+/\text{Cl}^-$  vs EC plot will remain consistent as EC increases. Fig. 8a reveals that only few samples during wet season follows evaporation trend line, which suggests that evaporation does not play a vital role in influencing the groundwater chemistry during wet season. However, an appreciable number of samples during dry season follow evaporation trend line, which signifies that evaporation could be among the factors influencing the groundwater chemistry during dry season.  $\text{Na}^+/\text{Cl}^-$  ratios shows significant correlation in wet and dry seasons.  $\text{Na}^+/\text{Cl}^-$  ratios enrichment and depletion was observed, which is an indicative of the influence of ion exchange and silicate dissolution in groundwater chemistry in respective seasons. However, most of the groundwater samples in the respective seasons deviated from 1:1 section. This suggests that  $\text{Ca}^{2+}$  is being exchanged for  $\text{Na}^+$  from clay minerals into water thereby increasing its salinity levels (Elumalai et al., 2022; Hu et al., 2024).

#### 4.5.3. Carbonate dissolution

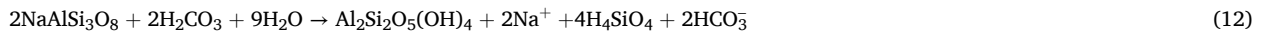
Carbonate minerals dissolution in groundwater produces  $\text{Ca}^{2+}$ ,  $\text{Mg}^{2+}$ , and  $\text{HCO}_3^-$  ions (Elumalai et al., 2022; Rajesh et al., 2012; Rajmohan et al., 2017; Rajmohan and Elango, 2004). Molar ratio of  $\text{Ca}^{2+}/\text{Mg}^{2+}$  serves as a reliable indicator for calcite and dolomite dissolution processes within groundwater system. Dissolution of dolomite will maintain  $\text{Ca}^{2+}/\text{Mg}^{2+}$  ratio of 1, but  $\text{Ca}^{2+}/\text{Mg}^{2+}$  ratio  $> 1$  indicates dissolution of calcite, and the process of silicate weathering is associated with  $\text{Ca}^{2+}/\text{Mg}^{2+}$  ratios  $> 2$  (Rajesh et al., 2012; Rajmohan et al., 2017). It is noteworthy that about 81.67 % and 73.33 % of the respective seasons groundwater have  $\text{Ca}^{2+}/\text{Mg}^{2+}$  ratio  $> 2$  (Fig. 8c). This implies that the groundwater samples are dominated by silicate weathering processes. Some portions of samples were observed to cluster between values of 1 and 2 on the  $\text{Ca}^{2+}/\text{Mg}^{2+}$  ratio scale, suggesting the dissolution of calcite which was described in Eq. (5). Moreover, the samples exhibited spatial distribution, and few samples were closely aligned with the  $\text{Ca}^{2+}/\text{Mg}^{2+} = 1$  line. This implies occurrence of high magnesium carbonate dissolution, which is expressed by the following equation (Eq. (11)):



#### 4.5.4. Silicate weathering

High  $\text{Na}^+$  in groundwater could be related to silicate rock weathering. According to Jankowski and Ian Acworth, (1997),  $\text{Na}^+/\text{Cl}^-$  ratio remains constant if evaporation is the prevailing mechanism in the absence of mineral precipitation. The dissolution of halite can result in  $\text{Na}^+/\text{Cl}^-$  ratio = 1 if present, however,  $\text{Na}^+/\text{Cl}^-$  ratio  $> 1$  increases  $\text{Na}^+$  concentration in groundwater system due to silicate weathering and cation exchange processes. Fig. 8a presents  $\text{Na}^+/\text{Cl}^-$  vs EC for wet and dry seasons in Komadugu–Yobe basin. A significant increase in  $\text{Na}^+/\text{Cl}^-$  ratio is observed when electrical conductivity (EC) value is below 500, particularly in wet season groundwater samples. It was observed that 78.33 % and 71.67 % of respective wet and dry season samples exhibited  $\text{Na}^+/\text{Cl}^- > 1$ . This high  $\text{Na}^+$  ion concentration could potentially originates from silicate weathering and/or cation exchange process (Fig. 8a). Furthermore,  $\text{Na}^+/\text{Cl}^-$  and EC plots shows significant number of samples above evaporation line, particularly in wet season. However, few dry season samples were observed in evaporation zone. Therefore, silicate weathering with ion exchange is likely the primary processes that controls the chemistry of groundwater during both seasons (Abu et al., 2024a and 2024b; Yang et al., 2024).

According to Rogers, (1989), if sodium is likely from silicate weathering by soil  $\text{CO}_2$ , groundwater would have bicarbonate ( $\text{HCO}_3^-$ ) as the predominant anion. The release of  $\text{HCO}_3^-$  is attributed to the reaction between feldspar crystals and carbonic acid in water.  $\text{HCO}_3^-$  is the prevailing anionic species found in groundwater of the study area (Table 1). Bivariate ratio plots indicate that silicate weathering is the primary geochemical process influencing groundwater chemistry in the basin, rather than carbonate and evaporite dissolution (Fig. 8d & e). Geochemical evolution of groundwater is characterized by silicate weathering, carbonate dissolution, cation exchange, and evaporative dissolution (Adimalla and Taloor, 2020; Banda et al., 2020; Elumalai et al., 2020, 2022; Ganyaglo et al., 2024; Liu et al., 2023; Rajesh et al., 2012; Rajmohan et al., 2017; Rajmohan and Elango, 2004; Sikakwe and Eyong, 2022; Singh et al., 2017; Yang et al., 2024). Impact of evaporite dissolution appears to be limited in the basin. However, it is visible in few locations during the dry season. This observation is indicative of prevalence of silicate source rocks and limited presence of evaporites, such as halite and gypsum. The latter are commonly related to deposits characterized by poorer permeability, inadequate flushing, and the presence of shale or marl (Banda et al., 2020; Yuan et al., 2024). The process of silicate weathering can be explained using the following weathering reaction (Eq. (12)):



#### 4.5.5. Ion exchange reactions

Ion exchange and different weathering processes are best described using  $\text{Na}^+/\text{Cl}^-$  vs. EC plot (Fig. 8a). The figure shows an increase in  $\text{Na}^+$  ion by ion exchange processes in water samples of both seasons. Therefore, cation exchange process is the predominant mechanisms that control the groundwater chemistry in the respective wet and dry seasons compared to reverse ion exchange. Ion exchange processes in aquifer system have been explained in several studies using chloroalkaline indices (CAI-I and CAI-II) (Eq. (3) & (4)). Positive values of chloroalkaline indices indicate the occurrence of reverse ion exchange, whereas negative values indicate cation exchange reaction (Abu et al., 2024a and 2024b; Elumalai et al., 2022; Mgbenu and Egbueri, 2019). High  $\text{Cl}^-$  over  $\text{Na}^+$  and  $\text{K}^+$  results in positive chloroalkaline indices, suggesting reverse ion exchange reactions. Conversely, high  $\text{Na}^+$  and  $\text{K}^+$  compared to  $\text{Cl}^-$  result in negative values, indicating cation exchange processes (Ganyaglo et al., 2024). When the values of chloroalkaline indices are positive,  $\text{Mg}^{2+}$  and  $\text{Ca}^{2+}$  ions are exchanged with  $\text{Na}^+$  and  $\text{K}^+$  ions in water. Conversely, when chloroalkaline indices have negative values, it suggest that there is exchange of  $\text{Mg}^{2+}$  or  $\text{Ca}^{2+}$  ions in groundwater with  $\text{Na}^+$  or  $\text{K}^+$  ions in host rocks. Fig. 8 f shows positive correlation between CAI-I and CAI-II. 86.67 % of the samples had negative chloroalkaline index values during the wet season, whereas 80 % had negative values during the dry season. However, 13.33 % and 20 % have positive values during the respective seasons confirming that cation exchange reaction is predominant in the groundwater system compared to reverse ion exchange process. Cation exchange can be explained in the following reactions (Eqs. (13) and (14)):



Where X is the cation exchange sites.

#### 4.6. Conceptual model for hydrogeochemical processes controlling the groundwater chemistry in Komadugu-Yobe basin

Fig. 9 presents a conceptual model for geochemical processes governing groundwater chemistry of Komadugu-Yobe basin. The study has established that the chemistry of groundwater in the basin is influenced by various geogenic and anthropogenic processes which indicates a subtle transformation as groundwater and surface water moves from upstream section passing through recharge zones in Hadejia Nguru wetlands to downstream parts along Komadugu Yobe river to Lake Chad. The study area is mainly characterized by local gravity driven flow due to varying topography from upstream to downstream. The aquifer in the upstream parts of the basin consists of a system of three aquifer layers resting on the Precambrian basement formation. The weathered basement which is semi-permeable in the vadose zone which hosted the water table. The partially weathered basement and the fractured basements provides groundwater in fractures, fault breccias, and joints which moves from upstream to downstream direction following natural slope of the bedrock. Localized infiltration from Chalawa gorge dam, river flows, industrial discharges, irrigation return flows and

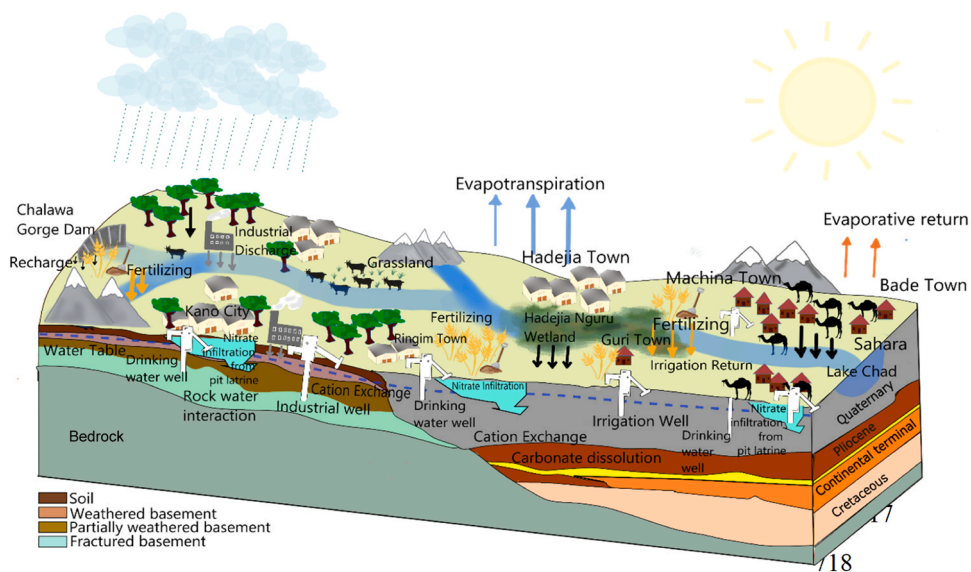


Fig. 9. Conceptual model for geochemical evolution and hydrogeochemical processes controlling the groundwater chemistry in Komadugu-Yobe basin.

domestic waste discharges as well as rock-water interaction influenced the groundwater chemistry and its evolution in upstream parts of the basin. The hydrochemical evolution shows that Ca-HCO<sub>3</sub> and Na-Cl water types predominated the region due to weathering/dissolution of Ca and Na bearing silicate minerals and calcite coupled with various anthropogenic inputs. Nitrate in the irrigation and residential areas may come from nitrogenous fertilizing and unimproved pit latrines respectively. However, in the downstream part of the study area, sedimentary quaternary aquifer provides groundwater mostly in unconfined aquifers. Groundwater occurs at shallow depth around Hadejia, Ringim and Guri town while it is at deeper depth in Machina town and its surroundings. Fig. 9 shows that groundwater in this region is recharged by infiltrating water in the Hadejia-Nguru wetland (HNW), Komadugu-Yobe valley and areas around Lake Chad. However, evapotranspiration occurs around HNW and farmlands as well as evaporation losses at the verge of downstream parts towards Lake Chad. The groundwater chemistry is highly impacted by anthropogenic activities rather than geogenic processes. Nitrate infiltrates into the subsurface from irrigation return flows, domestic waste discharges and unimproved pit latrines in the region.

## 5. Implications to groundwater sustainability

This study has successfully used a robust approach of geochemical modeling, bivariate plots, ionic ratios, and chemometric analysis and established the sources of chemical constituent influencing the general chemistry and geochemical evolution of groundwater in the transboundary Komadugu–Yobe basin, Lake Chad region. This information is crucial in developing groundwater monitoring and sustainable strategies for effective use and management of the basin's groundwater resources. Insights on the sources of chemical constituents in groundwater of the study area provides an avenue for understanding complex interplay between geogenic and anthropogenic factors influencing groundwater chemistry as well as groundwater evolution and hydrogeochemical characteristics for policy implementation as follows:

- The insights identified in this study regarding the sources of chemical constituents in groundwater are fundamental in providing strategic guides in developing and implementing effective policies for sustainable use and management of water resources. This would offer a more protective measures in ensuring healthy groundwater quality, particularly in areas prone to water contamination which is in line with SDG6 targets.
- Knowledge of various groundwater types in the study area and their distinct characteristics coupled with hydrochemical characteristics might influence decision on groundwater development projects in the region. Stringent policies should be implemented in areas at risk of contamination due to overexploitation or pollution from natural and anthropogenic sources.
- The Government of Nigeria should actively participate in the regional developmental projects being conducted by Lake Chad Basin Commission (LCBC) within Lake Chad region in restoring and safeguarding Lake Chad that provides a substantial groundwater recharge zones to the region's aquifers. These projects are essential in ensuring sustainable groundwater management and safeguarding water resources for the present population and the unborn generation.
- A significant percentage of potassium concentration due to incongruent weathering of potassium feldspar in the Precambrian basement region and nitrate contamination by irrigation return flows and pit latrines in irrigated and residential areas, as illustrated in Fig. 9 necessitates the development of detailed irrigation master plan and pollution model specifically addressing nitrate contamination from intensive synthetic fertilizing, pit latrines and sewerage systems. These activities would enable a more detailed analysis of nitrate-related contamination and support the establishment of stringent policies for proper land use planning to mitigate the potential health risk posed by nitrate in drinking groundwater.
- This study has undoubtedly provided an avenue for future research that would focus on trace element contamination and its associated health risk as well as the application isotope hydrology to understand groundwater recharge source/origin and possibly tracing various groundwater pollution sources.

## 6. Conclusion

This study employed an integrated approach of geochemical modeling, bivariate plots, ionic ratios, and chemometric analysis to explore geochemical evolution and mechanisms controlling the groundwater chemistry as well as origin/sources of chemical constituents in groundwater of the transboundary KYB. The groundwater in the basin is subjected to increased exploitation coupled with contamination from geogenic and anthropogenic inputs. The following conclusion can be drawn from the study:

- The Pearson's correlation analysis showed a positive relationship between EC and major ions, except with pH and Fe in the wet season and pH and F<sup>-</sup> in the dry season.
- Nitrate significantly correlated with all variables in the dry season, possibly due to excessive use of synthetic fertilizer during irrigation and nitrification from pit latrines.
- PCA results indicate that groundwater samples in PC1 were influenced by geogenic and anthropogenic sources, PC2 indicated the influence of agricultural and domestic waste inputs, while PC3 suggests fluoride enrichment due to mineral weathering and industrial activities.
- The R-mode HCA identified three cluster groups influenced by: both geogenic and anthropogenic factors (Cluster I); synthetic fertilizers and nitrification from pit latrines (Cluster II); and interactions among various geochemical processes (Cluster III).
- Q-mode HCA identified three water types with increasing mineralization levels influenced by geogenic, anthropogenic, and evaporation processes.



- Piper diagrams indicated Ca-HCO<sub>3</sub>, Na-Cl, and mixed water types, suggesting that groundwater is influenced by mineral weathering, ion exchange, and evaporation processes.
- Gibbs plots, bivariate plots, molar ratios, and chloroalkaline indices (CAI-I, CAI-II) confirms that the groundwater chemistry is influenced by geochemical processes like mineral weathering, evaporation, and ion exchange processes.
- Saturation indices revealed that most samples were undersaturated with respect to dolomite, calcite, and fluorite, as a result of carbonate precipitation.
- A significant percentage of groundwater samples (96.7 % in wet and 99.2 % in dry season) had partial pressure of CO<sub>2</sub> above atmospheric pCO<sub>2</sub> levels, as a source of acid for mineral dissolution.
- The study proves that geochemical modeling and chemometric analysis are effective techniques for assessing geochemical mechanisms and various chemical constituents within aquifer systems characterized by diverse contamination sources.
- Recommendations from the study include detailed trace element analysis and their associated health risk assessments, as well as isotope hydrology studies to identify groundwater recharge sources and contamination, supporting efficient groundwater management to mitigate significant risks to human health.

### CRedit authorship contribution statement

**Abdulrahman Shuaibu:** Writing – review & editing, Writing – original draft, Validation, Software, Resources, Project administration, Methodology, Investigation, Funding acquisition, Formal analysis, Data curation, Conceptualization. **Robert M Kalin:** Writing – review & editing, Validation, Supervision, Funding acquisition, Conceptualization. **Vernon Phoenix:** Writing – review & editing, Validation, Supervision, Funding acquisition. **Ibrahim Mohammed Lawal:** Writing – review & editing, Visualization, Validation, Software.

### Declaration of Competing Interest

The authors declare that they have no known competing financial interests or personal relationships that could have appeared to influence the work reported in this paper.

### Acknowledgements

Abdulrahman Shuaibu is grateful to the Petroleum Technology and Development Fund (PTDF) under the Overseas PhD scholarship scheme for providing financial support. The authors are thankful for financial support of the Scottish Government under the Climate Justice Fund Water Futures Program (research grant HN-CJF-03), awarded to the University of Strathclyde (Prof. R.M. Kalin), and to the IAEA RAF7021 programme for access to regional data.

### Appendix A. Supporting information

Supplementary data associated with this article can be found in the online version at [doi:10.1016/j.ejrh.2024.102098](https://doi.org/10.1016/j.ejrh.2024.102098).

### Data availability

Data will be made available on request.

### References

- Abdelaziz, S., Gad, M.I., El Tahan, A.H.M.H., 2020. Groundwater quality index based on PCA: Wadi El-Natrun, Egypt. *J. Afr. Earth Sci.* 172 (October 2019), 103964. <https://doi.org/10.1016/j.jafrearsci.2020.103964>.
- Abu, M., Akurugu, B.A., Egbueri, J.C., 2024a. Understanding groundwater mineralization controls and the implications on its quality (Southwestern Ghana): insights from hydrochemistry, multivariate statistics, and multi-linear regression models. *Acta Geophys.* 72 (5), 3563–3580. <https://doi.org/10.1007/s11600-023-01271-6>.
- Abu, M., Zango, M.S., Kazapoe, R.W., 2024b. Controls of groundwater mineralization assessment in a mining catchment in the Upper West Region, Ghana: insights from hydrochemistry, pollution indices of groundwater, and multivariate statistics. *Innov. Green. Dev.* 3 (1), 100099. <https://doi.org/10.1016/j.igd.2023.100099>.
- Abubakar, I.T., Maharazu, A.Y., Emmanuel, A.O., Adnan, A., 2018. Shallow groundwater condition for irrigation along dryland river basin, northwestern Nigeria. *J. Dryland Agric.* 4 (1), 1–11. <https://doi.org/10.5897/joda2018.0003>.
- Adams, S., Titus, R., Pietersen, K., Tredoux, G., Harris, C., 2001. Hydrochemical characteristics of aquifers near Sutherland in the Western Karoo, South Africa. *J. Hydrol.* 241 (1–2), 91–103. [https://doi.org/10.1016/S0022-1694\(00\)00370-X](https://doi.org/10.1016/S0022-1694(00)00370-X).
- Adeyeri, O.E., Lamptey, B.L., Lawin, A.E., Sanda, I.S., 2017. Spatio-temporal precipitation trend and homogeneity analysis in Komadugu-Yobe Basin, Lake Chad Region. *J. Climatol. Weather Forecast.* 05 (03). <https://doi.org/10.4172/2332-2594.1000214>.
- Adeyeri, O.E., Laux, P., Lawin, A.E., Ige, S.O., Kunstmann, H., 2020. Analysis of hydrometeorological variables over the transboundary komadugu-yobe basin, West Africa. *J. Water Clim. Change* 11 (4), 1339–1354. <https://doi.org/10.2166/wcc.2019.283>.
- Adeyeri, O.E., Laux, P., Lawin, A.E., Arnault, J., 2020. Assessing the impact of human activities and rainfall variability on the river discharge of Komadugu-Yobe Basin, Lake Chad Area. *Environ. Earth Sci.* 79 (6), 1–12. <https://doi.org/10.1007/s12665-020-8875-y>.

- Adeyeri, O.E., Lawin, A.E., Laux, P., Ishola, K.A., Ige, S.O., 2019. Analysis of climate extreme indices over the Komadugu-Yobe basin, Lake Chad region: past and future occurrences. *Weather Clim. Extrem.* 23 (January), 100194. <https://doi.org/10.1016/j.wace.2019.100194>.
- Adimalla, N., Taloor, A.K., 2020. Hydrogeochemical investigation of groundwater quality in the hard rock terrain of South India using Geographic Information System (GIS) and groundwater quality index (GWQI) techniques. *Groundw. Sustain. Dev.* 10 (126), 100288. <https://doi.org/10.1016/j.gsd.2019.100288>.
- Ahmed, S.D., Agodzo, S.K., Adjei, K.A., Deinmodei, M., Ameso, V.C., 2018. Preliminary investigation of flooding problems and the occurrence of kidney disease around Hadejia-Nguru wetlands, Nigeria and the need for an ecohydrology solution. *Ecohydrol. Hydrobiol.* 18 (2), 212–224. <https://doi.org/10.1016/j.ecohyd.2017.11.005>.
- Ait Said, B., Mili, E.M., El Faleh, E.M., Mehdaoui, R., Mahboub, A., Hamid, F.E., Tlemcani, J., El Fakir, R., 2023. Hydrochemical evolution and groundwater quality assessment of the Tinejad-Touroug quaternary aquifer, South-East Morocco. *Front. Ecol. Evol.* 11 (September), 1–21. <https://doi.org/10.3389/fevo.2023.1201748>.
- APHA. (2012). AWWA, WEF. Standard Methods for examination of water and wastewater. 22nd ed. Washington: American Public Health Association; 2012, 1360 pp. ISBN 978-087553-013-0 (<http://www.standardmethods.org/>). *Washington: APHA*, 5(3), 335.
- Asomaning, J., Ofosu, E., Laar, C., Saka, D., 2023. Statistical and isotopic analysis of sources and evolution of groundwater. *Phys. Chem. Earth* 129 (ember 2022), 103337. <https://doi.org/10.1016/j.pce.2022.103337>.
- Awaleh, M.O., Boschetti, T., Ahmed, M.M., Dabar, O.A., Robleh, M.A., Waberi, M.M., Ibrahim, N.H., Dirieh, E.S., 2024. Spatial distribution, geochemical processes of high-content fluoride and nitrate groundwater, and an associated probabilistic human health risk appraisal in the Republic of Djibouti. *Sci. Total Environ.* 927 (March), 171968. <https://doi.org/10.1016/j.scitotenv.2024.171968>.
- Banda, L.C., Kalin, R.M., Phoenix, V., 2024. Isotope hydrology and hydrogeochemical signatures in the resource conceptualisation. *Water* 16, 1587. <https://doi.org/10.3390/w16111587>.
- Banda, L.C., Zavison, A.S.K., Phiri, P., Kamtukle, S., Rivett, M.O., Kalin, R.M., Kapachika, C., Fraser, C., 2020. Seasonally variant stable isotope baseline characterisation of Malawi's Shire river basin to support integrated water resources 2020 management. *Water* 12, 1410. <https://doi.org/10.3390/w12051410>.
- Beshir, A., Reddythota, D., Alemayehu, E., 2024. Evaluation of drinking water quality and associated health risks in Adama City, Ethiopia. *Heliyon* 10 (16), e36363. <https://doi.org/10.1016/j.heliyon.2024.e36363>.
- Bijay-Singh, Craswell, E., 2021. Fertilizers and nitrate pollution of surface and ground water: an increasingly pervasive global problem. *SN Appl. Sci.* 3 (4), 1–24. <https://doi.org/10.1007/s42452-021-04521-8>.
- Bradai, A., Yahiaoui, I., Douaoui, A., Abdennour, M.A., Gulakhmadov, A., Chen, X., 2022. Combined modeling of multivariate analysis and geostatistics in assessing groundwater irrigation sustenance in the middle Chelif Plain (North Africa). *Water (Switz.)* 14 (6). <https://doi.org/10.3390/w14060924>.
- Bura, B., Goni, I.B., Sheriff, B.M., Gazali, A.K., 2018. Occurrence and distribution of fluoride in groundwater of chad formation aquifers in Borno state, Nigeria. *Int. J. Hydrol.* 2 (4), 528–537. <https://doi.org/10.15406/ijh.2018.02.00121>.
- Carter, R.C., Alkali, A.G., 1996. Shallow groundwater in the northeast arid zone of Nigeria. *Q. J. Eng. Geol.* 29 (4), 341–355. <https://doi.org/10.1144/GSL.QJEGH.1996.029.P4.07>.
- Chen, S., Tang, Z., Wang, J., Wu, J., Yang, C., Kang, W., Huang, X., 2020. Multivariate analysis and geochemical signatures of shallow groundwater in the main urban area of chongqing, southwestern china. *Water* 12 (10). <https://doi.org/10.3390/w12102833>.
- Chen, W., Wu, C., Pan, S., Shi, L., 2024. Analysis on the spatiotemporal evolutions of groundwater hydrochemistry and water quality caused by over-extraction and seawater intrusion in eastern coastal China. *Front. Earth Sci.* 12 (April), 1–17. <https://doi.org/10.3389/feart.2024.1391235>.
- Dasari, B.M., Aradhi, K.K., Banothu, D., Kurakalva, R.M., 2024. Assessment of groundwater quality, source identification, and health risk around oil and gas drilling sites. In: *Environmental Earth Sciences*, 83. Springer, Berlin Heidelberg. <https://doi.org/10.1007/s12665-024-11576-4>.
- Desclotres, M., Chalikakis, K., Legchenko, A., Moussa, A.M., Genthon, P., Favreau, G., Le Coz, M., Boucher, M., Oi, M., 2013. Investigation of groundwater resources in the Komadugu Yobe Valley (Lake Chad Basin, Niger) using MRS and TDEM methods. *J. Afr. Earth Sci.* 87, 71–85. <https://doi.org/10.1016/j.jafrearsci.2013.07.006>.
- Dhaoui, O., Antunes, I.M.H.R., Boente, C., Agoubi, B., Kharroubi, A., 2023. Hydrogeochemical processes on inland aquifer systems: a combined multivariate statistical technique and isotopic approach. *Groundw. Sustain. Dev.* 20 (December 2022), 100887. <https://doi.org/10.1016/j.gsd.2022.100887>.
- Ding, K., Zhang, Y., Zhang, H., Yu, C., Li, X., Zhang, M., Zhang, Z., Yang, Y., 2024. Tracing nitrate origins and transformation processes in groundwater of the Hohhot Basin's Piedmont strong runoff zone through dual isotopes and hydro-chemical analysis. *Sci. Total Environ.* 919 (February), 170799. <https://doi.org/10.1016/j.scitotenv.2024.170799>.
- Elumalai, V., Nethononda, V.G., Manivannan, V., Rajmohan, N., Li, P., Elango, L., 2020. Groundwater quality assessment and application of multivariate statistical analysis in Luvuvhu catchment, Limpopo, South Africa. *J. Afr. Earth Sci.* 171 (August), 103967. <https://doi.org/10.1016/j.jafrearsci.2020.103967>.
- Elumalai, V., Nwabisa, D.P., Rajmohan, N., 2019. Evaluation of high fluoride contaminated fractured rock aquifer in South Africa – Geochemical and chemometric approaches. *Chemosphere* 235, 1–11. <https://doi.org/10.1016/j.chemosphere.2019.06.065>.
- Elumalai, V., Rajmohan, N., Sithole, B., Li, P., Uthandi, S., van Tol, J., 2022. Geochemical evolution and the processes controlling groundwater chemistry using ionic ratios, geochemical modelling and chemometric analysis in a semi-arid region of South Africa. *Chemosphere* 312 (P11), 137179. <https://doi.org/10.1016/j.chemosphere.2022.137179>.
- Gana, B.A., Harir, A.I., Bogoro, A.G., & Oladosu, R.O. (2018). Stream Ordering As a Tool For Effective River Basin Development: Examples From Komadugu – Yobe River Basin.. 44(May 2019), 67–78.
- Ganyaglo, S.Y., Binyiako, J.Y., Teye, E.M., Gibrilla, A., Abdul-Wahab, D., Edusei, S., Amponsah, P., Egbi, C.D., Dampare, S.B., Asare, E.A., 2024. Groundwater geochemical evolution, origin and quality in the Lower Pra Basin, Ghana: insights from hydrogeochemistry, multivariate statistical analysis, mineral saturation indices, stable isotopes ( $\delta^2\text{H}$  and  $\delta^{18}\text{O}$ ) and geostatistical analysis. *Acta Geochim.* 0123456789. <https://doi.org/10.1007/s11631-024-00725-y>.
- Garba, Y.I., Gano, U.T., Yusuuf, M.S., Musa, D.M., 2018. Assessment of physicochemical and microbial quality of borehole water in Dutse metropolis Jigawa State, Nigeria. *Sci. World J.* 13 (3), 1–5.
- Gautam, A., Rai, S.C., Rai, S.P., Ram, K., Sanny, 2022. Impact of anthropogenic and geological factors on groundwater hydrochemistry in the unconfined aquifers of Indo-Gangetic plain. *Phys. Chem. Earth* 126 (July 2021), 103109. <https://doi.org/10.1016/j.pce.2022.103109>.
- Gibbs, J.R., 1970. Mechanisms controlling world water chemistry. *Science* 170 (3962), 1088–1090. <https://doi.org/10.1126/science.170.3962.1088>.
- Goes, B.J.M., 1999. Estimate of shallow groundwater recharge in the Hadejia-Nguru Wetlands, semi-arid northeastern Nigeria. *Hydrogeol. J.* 7 (3), 294–304. <https://doi.org/10.1007/s100400050203>.
- Goni, I.B., 2006. Tracing stable isotope values from meteoric water to groundwater in the southwestern part of the Chad basin. *Hydrogeol. J.* 14 (5), 742–752. <https://doi.org/10.1007/s10040-005-0469-y>.
- Goni, I.B., Sheriff, B.M., Kolo, A.M., Ibrahim, M.B., 2019. Assessment of nitrate concentrations in the shallow groundwater aquifer of Maiduguri and environs, Northeastern Nigeria. *Sci. Afr.* 4, e00089. <https://doi.org/10.1016/j.sciaf.2019.e00089>.
- Goni, I., Vassolo, S., Sheriff, M., Aji, M., Bura, B., Ibrahim, Y., 2023. Geochemical and isotopic studies in parts of the Hadejia-Jamaare-Komadugu-Yobe Basin, NE Nigeria. *Hydrogeol. J.* 0123456789. <https://doi.org/10.1007/s10040-023-02637-2>.
- Ha, Q.K., Tran Ngoc, T.D., Le Vo, P., Nguyen, H.Q., Dang, D.H., 2022. Groundwater in Southern Vietnam: Understanding geochemical processes to better preserve the critical water resource. *Sci. Total Environ.* 807, 151345. <https://doi.org/10.1016/j.scitotenv.2021.151345>.
- Hamidu, H., Falalu, B.H., Abdullahi, I.M., Kwaya, M.Y., Arabi, A.S., 2017. Groundwater chemistry, storage and dynamics in parts of Jigawa Central, Northwestern Nigeria. *Bayero J. Pure Appl. Sci.* 10 (1), 138. <https://doi.org/10.4314/bajopas.v10i1.19>.
- Hu, W., Xiao, Y., Wang, L., Zhang, Y., Feng, M., Shi, W., He, C., Wen, Y., Yang, H., Han, J., Wang, J., 2024. Spatial variability, source identification, and partitioning of groundwater constituents in a typical lakeside plain on Yungui Plateau. *Process Saf. Environ. Prot.* 191 (PB), 2402–2415. <https://doi.org/10.1016/j.psep.2024.09.107>.
- Ibrahim, A., Suleiman, A.A., Abdullahi, U.A., Suleiman, S.A., 2021. Monitoring groundwater quality using probability distribution in Gwale, Kano state, Nigeria. *J. Stat. Model. Anal.* 3 (2), 95–108. <https://doi.org/10.22452/josma.vol3no2.6>.

- Ismail, A.H., Hassan, G., Sarhan, A.H., 2020. Hydrochemistry of shallow groundwater and its assessment for drinking and irrigation purposes in Tarmiah district, Baghdad governorate, Iraq. *Groundw. Sustain. Dev.* 10 (November 2019), 100300. <https://doi.org/10.1016/j.gsd.2019.100300>.
- Jabbo, J.N., Isa, N.M., Aris, A.Z., Ramli, M.F., Abubakar, M.B., 2022. Geochemometric approach to groundwater quality and health risk assessment of heavy metals of Yankari Game Reserve and its environs, Northeast Nigeria. *J. Clean. Prod.* 330 (February 2021), 129916. <https://doi.org/10.1016/j.jclepro.2021.129916>.
- Jagaba, A.H., Kutty, S.R.M., Hayder, G., Baloo, L., Abubakar, S., Ghaleb, A.A.S., Lawal, I.M., Noor, A., Umaru, I., Almahbashi, N.M.Y., 2020. Water quality hazard assessment for hand dug wells in Rafin Zurfi, Bauchi State, Nigeria. *Ain Shams Eng. J.* 11 (4), 983–999. <https://doi.org/10.1016/j.asej.2020.02.004>.
- Jankowski, J., Ian Acworth, R., 1997. Impact of debris-flow deposits on hydrogeochemical process and the development of dry land salinity in the Yass River catchment, New South Wales, Australia. *Hydrogeol. J.* 5 (4), 71–88. <https://doi.org/10.1007/s100400050119>.
- Jehan, S., Khan, S., Khattak, S.A., Muhammad, S., Rashid, A., Muhammad, N., 2019. Hydrochemical properties of drinking water and their sources apportionment of pollution in Bajaur agency, Pakistan. *Meas.: J. Int. Meas. Confed.* 139, 249–257. <https://doi.org/10.1016/j.measurement.2019.02.090>.
- Kalin, R., 1996. Basic concepts and formulations for isotope geochemical modelling of groundwater systems. IAEA-TECDOC-910 Manual on Mathematical Models in Isotope Hydrogeology. IAEA.
- Kalin, R.M., Long, A., 1993. Application of hydrogeochemical modelling for validation of hydrologic flow modelling in the Tucson basin aquifer, Arizona, United States of America. *Math. Models Their Appl. Isot. Stud. Groundw. Hydrol.*, June 147–178.
- Karmakar, B., Singh, M.K., Choudhary, B.K., Singh, S.K., Egbueri, J.C., Gautam, S.K., Rawat, K.S., 2023. Investigation of the hydrogeochemistry, groundwater quality, and associated health risks in industrialized regions of Tripura, northeast India. *Environ. Forensics* 24 (5–6), 285–306. <https://doi.org/10.1080/15275922.2021.2006363>.
- Khan, A., Naem, M., Zekker, I., Arian, M.B., Michalski, G., Khan, A., Shah, N., Zeeshan, S., ul Haq, H., Subhan, F., Ikram, M., Shah, M.I.A., Khan, I., Shah, L.A., Zahoor, M., Khurshed, A., 2023. Evaluating groundwater nitrate and other physicochemical parameters of the arid and semi-arid district of DI Khan by multivariate statistical analysis. *Environ. Technol.* 44 (7), 911–920. <https://doi.org/10.1080/09593330.2021.1987532>.
- Kumar, S., Venkatesh, A.S., Singh, R., Udayabhanu, G., Saha, D., 2018. Geochemical signatures and isotopic systematics constraining dynamics of fluoride contamination in groundwater across Jamui district, Indo-Gangetic alluvial plains, India. *Chemosphere* 205, 493–505. <https://doi.org/10.1016/j.chemosphere.2018.04.116>.
- Le Coz, M., Genthon, P., Adler, P.M., 2011. Multiple-point statistics for modeling facies heterogeneities in a porous medium: the Komadugu-Yobe Alluvium, Lake Chad Basin. *Math. Geosci.* 43 (7), 861–878. <https://doi.org/10.1007/s11004-011-9353-6>.
- Lima, I.Q., Muñoz, M.O., Ramos, O.E.R., Bhattacharya, P., Choque, R.Q., Aguirre, J.Q., Sracek, O., 2019. Hydrochemical assessment with respect to arsenic and other trace elements in the Lower Katari Basin, Bolivian Altiplano. *Groundw. Sustain. Dev.* 8 (September 2018), 281–293. <https://doi.org/10.1016/j.gsd.2018.11.013>.
- Liu, F., Song, X., Yang, L., Zhang, Y., Han, D., Ma, Y., Bu, H., 2015. Identifying the origin and geochemical evolution of groundwater using hydrochemistry and stable isotopes in the Subei Lake basin, Ordos energy base, Northwestern China. *Hydrol. Earth Syst. Sci.* 19 (1), 551–565. <https://doi.org/10.5194/hess-19-551-2015>.
- Liu, F., Zhang, J., Wang, S., Zou, J., Zhen, P., 2023. Multivariate statistical analysis of chemical and stable isotopic data as indicative of groundwater evolution with reduced exploitation. *Geosci. Front.* 14 (1), 101476. <https://doi.org/10.1016/j.gsf.2022.101476>.
- Liu, F., Zhao, Z., Yang, L., Ma, Y., Xu, Y., Gong, L., Liu, H., 2020. Geochemical characterization of shallow groundwater using multivariate statistical analysis and geochemical modeling in an irrigated region along the upper Yellow River, Northwestern China. *J. Geochem. Explor.* 215 (April), 106565. <https://doi.org/10.1016/j.gexplo.2020.106565>.
- Loh, Y.S.A., Akurugu, B.A., Manu, E., Aliou, A.S., 2020. Assessment of groundwater quality and the main controls on its hydrochemistry in some Voltaian and basement aquifers, northern Ghana. *Groundw. Sustain. Dev.* 10 (May 2019), 100296. <https://doi.org/10.1016/j.gsd.2019.100296>.
- Maduabuchi, C., Faye, S., Maloszewski, P., 2006. Isotope evidence of palaeorecharge and palaeoclimate in the deep confined aquifers of the Chad Basin, NE Nigeria. *Sci. Total Environ.* 370 (2–3), 467–479. <https://doi.org/10.1016/j.scitotenv.2006.08.015>.
- Memon, Y.I., Qureshi, S.S., Kandhar, I.A., Qureshi, N.A., Saeed, S., Mubarak, N.M., Ullah Khan, S., Saleh, T.A., 2023. Statistical analysis and physicochemical characteristics of groundwater quality parameters: a case study. *Int. J. Environ. Anal. Chem.* 103 (10), 2270–2291. <https://doi.org/10.1080/03067319.2021.1890064>.
- Mgbenu, C.N., Egbueri, J.C., 2019. The hydrogeochemical signatures, quality indices and health risk assessment of water resources in Umunya district, southeast Nigeria. *Appl. Water Sci.* 9 (1), 1–19. <https://doi.org/10.1007/s13201-019-0900-5>.
- Mohamed, A., Asmoay, A., Alshehri, F., Abdelrady, A., Othman, A., 2022. Hydro-geochemical applications and multivariate analysis to assess the water-rock interaction in arid environments. *Appl. Sci.* 12 (13). <https://doi.org/10.3390/app12136340>.
- Mohammed, A.U., Aris, A.Z., Ramli, M.F., Isa, N.M., Arabi, A.S., Jabbo, J.N., 2023. Groundwater pollutants characterization by geochemometric technique and geochemical modeling in tropical savanna watershed. *Environ. Geochem. Health* 45 (6), 3891–3906. <https://doi.org/10.1007/s10653-022-01468-6>.
- Mohammed, M.A.A., Szabó, N.P., Szűcs, P., 2022. Multivariate statistical and hydrochemical approaches for evaluation of groundwater quality in north Bahri city-Sudan. *Heliyon* 8 (11), e11308. <https://doi.org/10.1016/j.heliyon.2022.e11308>.
- Nyambar, I.N. anak, Mohan Viswanathan, P., 2024. Assessment on urban lakes along the coastal region of Miri, NW Borneo: implication for hydrochemistry, water quality, and pollution risk. *Environ. Sci. Pollut. Res.* 31 (29), 41306–41328. <https://doi.org/10.1007/s11356-023-25172-9>.
- Obaje, N.G., Wehner, H., Hamza, H., Scheeder, G., 2004. New geochemical data from the Nigerian sector of the Chad basin: implications on hydrocarbon prospectivity. *J. Afr. Earth Sci.* 38 (5), 477–487. <https://doi.org/10.1016/j.jafrearsci.2004.03.003>.
- Piper, A.M., 1944. A graphic procedure in the geochemical interpretation of water-analyses. *Trans. Am. Geophys Union* 25 (6), 914–928. <https://doi.org/10.1029/TR0251006p00914>.
- Rajesh, R., Brindha, K., Murugan, R., Elango, L., 2012. Influence of hydrogeochemical processes on temporal changes in groundwater quality in a part of Nalgonda district, Andhra Pradesh, India. *Environ. Earth Sci.* 65 (4), 1203–1213. <https://doi.org/10.1007/s12665-011-1368-2>.
- Rajmohan, N., Elango, L., 2004. Identification and evolution of hydrogeochemical processes in the groundwater environment in an area of the Palar and Cheyyar River Basins, Southern India. *Environ. Geol.* 27 (1), 47–61. <https://doi.org/10.1007/s00254-004-1012-5>.
- Rajmohan, N., Masoud, M.H.Z., Niyazi, B.A.M., 2021. Impact of evaporation on groundwater salinity in the arid coastal aquifer, Western Saudi Arabia. *Catena* 196 (April 2020), 104864. <https://doi.org/10.1016/j.catena.2020.104864>.
- Rajmohan, N., Patel, N., Singh, G., Amarasinghe, U.A., 2017. Hydrochemical evaluation and identification of geochemical processes in the shallow and deep wells in the Ramganga Sub-Basin, India. *Environ. Sci. Pollut. Res.* 24 (26), 21459–21475. <https://doi.org/10.1007/s11356-017-9704-z>.
- Rezaei, A., Hassani, H., Tziritis, E., Fard Mousavi, S.B., Jabbari, N., 2020. Hydrochemical characterization and evaluation of groundwater quality in Dalgan basin, SE Iran. *Groundw. Sustain. Dev.* 10 (December 2019), 100353. <https://doi.org/10.1016/j.gsd.2020.100353>.
- Rogers, J.R. (1989). Geochemical comparison of groundwater in areas of New England, New York, and Pennsylvania. *Groundwater*, 27(5), 690–712. (<https://medium.com/@arifwicaksanaa/pengertian-use-case-a7e576e1b6bf>).
- Samtio, M.S., Hakro, A.A. alias D., Jahangir, T.M., Mastoi, A.S., Lanjwani, M.F., Rajper, R.H., Lashari, R.A., Agheem, M.H., Noonari, M.W., 2023. Impact of rock-water interaction on hydrogeochemical characteristics of groundwater: using multivariate statistical, water quality index and irrigation indices of chachro sub-district, thar desert, sindh, Pakistan. *Groundw. Sustain. Dev.* 20 (March 2022), 100878. <https://doi.org/10.1016/j.gsd.2022.100878>.
- Sarti, O., Otal, E., Morillo, J., Ouassini, A., 2021. Integrated assessment of groundwater quality beneath the rural area of R'mel, Northwest of Morocco. *Groundw. Sustain. Dev.* 14 (June). <https://doi.org/10.1016/j.gsd.2021.100620>.
- Schuster, M., Düringer, P., Ghienne, J.F., Roquin, C., Sepulchre, P., Moussa, A., Lebatard, A.E., Mackaye, H.T., Likius, A., Vignaud, P., Brunet, M., 2009. Chad Basin: paleoenvironments of the Sahara since the Late Miocene. *Comptes Rendus - Geosci.* 341 (8–9), 603–611. <https://doi.org/10.1016/j.crte.2009.04.001>.
- Sheng, D., Meng, X., Wen, X., Wu, J., Yu, H., Wu, M., 2022. Contamination characteristics, source identification, and source-specific health risks of heavy metal(loids) in groundwater of an arid oasis region in Northwest China. *Sci. Total Environ.* 841 (March), 156733. <https://doi.org/10.1016/j.scitotenv.2022.156733>.
- Shuaibu, A., Hounkpè, J., Bossa, A.Y., Kalin, R.M., 2022. Flood risk assessment and mapping in the hadejia river multi-criterion decision-making method. *Water* 14, 3709. <https://doi.org/10.3390/w14223709>.

- Shuaibu, A., Kalin, R.M., Phoenix, V., Banda, L.C., Lawal, I.M., 2024. Hydrogeochemistry and Water Quality Index for Groundwater Sustainability in the Komadugu-Yobe Basin, Sahel Region. *Water* 16 (601), 1–22. <https://doi.org/10.3390/w16040601>.
- Shuaibu, A., Mujahid Muhammad, M., Bello, A.A.D., Sulaiman, K., Kalin, R.M., 2023. Flood estimation and control in a micro-watershed using GIS-based integrated approach. *Water* 15 (24), 1–20. <https://doi.org/10.3390/w15244201>.
- Sikakwe, G.U., Eyong, G.A., 2022. Groundwater flow and geochemical processes affecting its quality in the basement (Oban Massif) and sedimentary (Mamfe Embayment) environments, southeastern Nigeria. *J. Afr. Earth Sci.* 188 (December 2021), 104467. <https://doi.org/10.1016/j.jafrearsci.2022.104467>.
- Sikakwe, G.U., Nwachukwu, A.N., Uwa, C.U., Abam Eyong, G., 2020. Geochemical data handling, using multivariate statistical methods for environmental monitoring and pollution studies. *Environ. Technol. Innov.* 18, 100645. <https://doi.org/10.1016/j.eti.2020.100645>.
- Singh, C.K., Kumar, A., Shashtri, S., Kumar, A., Kumar, P., Mallick, J., 2017. Multivariate statistical analysis and geochemical modeling for geochemical assessment of groundwater of Delhi, India. *J. Geochem. Explor.* 175, 59–71. <https://doi.org/10.1016/j.gexplo.2017.01.001>.
- Spellman, P., Pain, A., Breithaupt, C., Bremner, P.M., 2024. Using multivariate statistics to link major ion chemistry changes at karst springs to agriculture. *Sci. Total Environ.* 921 (February), 170573. <https://doi.org/10.1016/j.scitotenv.2024.170573>.
- Subba Rao, N., Chaudhary, M., 2019. Hydrogeochemical processes regulating the spatial distribution of groundwater contamination, using pollution index of groundwater (PIG) and hierarchical cluster analysis (HCA): a case study. *Groundw. Sustain. Dev.* 9 (May), 100238. <https://doi.org/10.1016/j.gsd.2019.100238>.
- Subba Rao, N., Dinakar, A., Sun, L., 2022. Estimation of groundwater pollution levels and specific ionic sources in the groundwater, using a comprehensive approach of geochemical ratios, pollution index of groundwater, unmix model and land use/land cover – A case study. *J. Contam. Hydrol.* 248 (April). <https://doi.org/10.1016/j.jconhyd.2022.103990>.
- Suleiman, A.A., Abdullahi, U.A., Suleiman, A., Suleiman, S.A., Abubakar, H.U., 2022. Correlation and regression model for physicochemical quality of groundwater in the Jaen District of Kano State, Nigeria. *J. Stat. Model. Anal.* 4 (1), 14–24. <https://doi.org/10.22452/josma.vol4no1.2>.
- Sunkari, E.D., Ididrisu, R., Turkson, J., Okyere, M.B., Ambushe, A.A., 2025. Hydrogeochemical evaluation of groundwater evolution and quality in some Voltaian aquifers of Kintampo South District, Bono East Region, Ghana: implications from chemometric analysis, geochemical modeling and geospatial mapping techniques. *HydroResearch* 8, 13–27. <https://doi.org/10.1016/j.hydres.2024.09.001>.
- Trabelsi, R., Zouari, K., 2019. Coupled geochemical modeling and multivariate statistical analysis approach for the assessment of groundwater quality in irrigated areas: a study from North Eastern of Tunisia. *Groundw. Sustain. Dev.* 8 (October 2017), 413–427. <https://doi.org/10.1016/j.gsd.2019.01.006>.
- Tukur, A.I., Nabegu, A.B., Umar, D.A., Olofin, E.A., Azmin Sulaiman, W.N., 2018. Groundwater condition and management in Kano region, Northwestern Nigeria. *Hydrology* 5 (1), 1–21. <https://doi.org/10.3390/hydrology5010016>.
- Tziritis, E., Sachsamnoglou, E., Güler, C., 2024. Evaluating spatiotemporal groundwater quality changes in the Rhodope coastal aquifer system (NE Greece) employing a GIS-assisted hybrid approach of multivariate statistics and inverse geochemical modeling. *Sci. Total Environ.* 947 (July), 174676. <https://doi.org/10.1016/j.scitotenv.2024.174676>.
- Ullah, H., Naz, I., Alhodaib, A., Abdullah, M., Muddassar, M., 2022. Coastal groundwater quality evaluation and hydrogeochemical characterization using chemometric techniques. *Water* 14 (21), 3583. <https://doi.org/10.3390/w14213583>.
- Wali, S.U., Alias, N.B., Harun, S.B., Umar, K.J., Gada, M.A., Dankani, I.M., Kaoje, I.U., Usman, A.A., 2022. Water quality indices and multivariate statistical analysis of urban groundwater in semi-arid Sokoto Basin, Northwestern Nigeria. *Groundw. Sustain. Dev.* 18 (August 2021), 100779. <https://doi.org/10.1016/j.gsd.2022.100779>.
- Wali, S.U., Dankani, I.M., Abubakar, S.D., Gada, M.A., Usman, A.A., Shera, I.M., Umar, K.J., 2020. Review of groundwater potentials and groundwater hydrochemistry of semi-arid Hadejia-Yobe Basin, North-eastern Nigeria. *J. Geol. Res.* 2 (2), 20–33. <https://doi.org/10.30564/jgr.v2i2.2140>.
- Wali, S.U., Umar, K.J., Abubakar, S.D., Ifabiye, I.P., Dankani, I.M., Shera, I.M., Yauri, S.G., 2019. Hydrochemical characterization of shallow and deep groundwater in Basement Complex areas of southern Kebbi State, Sokoto Basin, Nigeria. In: *Applied Water Science*, 9. Springer International Publishing. <https://doi.org/10.1007/s13201-019-1042-5>.
- Wang, P., Zhang, W., Zhu, Y., Liu, Y., Li, Y., Cao, S., Hao, Q., Liu, S., Kong, X., Han, Z., Li, B., 2024. Evolution of groundwater hydrochemical characteristics and formation mechanism during groundwater recharge: a case study in the Hutuo River alluvial-pluvial fan, North China Plain. *Sci. Total Environ.* 915 (3), 170159. <https://doi.org/10.1016/j.scitotenv.2024.170159>.
- Yadav, A., Nanda, A., Sahu, B.L., Sahu, Y.K., Patel, K.S., Pervez, S., Gulgundi, M.S., Cuchi-Oterino, J.A., Martín-Ramos, P., Bhattacharya, P., 2020. Groundwater hydrochemistry of Rajnandgaon district, Chhattisgarh, Central India. *Groundw. Sustain. Dev.* 11 (January). <https://doi.org/10.1016/j.gsd.2020.100352>.
- Yang, F., Liu, S., Jia, C., Gao, M., Chang, W., Wang, Y., 2021. Hydrochemical characteristics and functions of groundwater in southern Laizhou Bay based on the multivariate statistical analysis approach. *Estuar., Coast. Shelf Sci.* 250 (72), 107153. <https://doi.org/10.1016/j.ecss.2020.107153>.
- Yang, H., Xiao, Y., Yang, S., Zhao, Z., Wang, S., Xiao, S., Wang, J., Zhang, Y., Wang, J., Yuan, Y., Wang, N., Wang, L., Hu, W., 2024. Geochemical fingerprints, evolution, and driving forces of groundwater in an alpine basin on Tibetan Plateau: Insights from unsupervised machine learning and objective weight allocation approaches. *J. Hydrol.: Reg. Stud.* 56 (October), 102054. <https://doi.org/10.1016/j.ejrh.2024.102054>.
- Yu, D., Deng, J., Jiang, Q., Liu, H., Yu, C., Ma, H., Pu, S., 2024. Evaluation of groundwater quality with multi-source pollution based on source identification and health risks. *Sci. Total Environ.* 949 (December 2023), 175064. <https://doi.org/10.1016/j.scitotenv.2024.175064>.
- Yuan, Z., Jian, Y., Chen, Z., Jin, P., Gao, S., Wang, Q., Ding, Z., Wang, D., Ma, Z., 2024. Distribution of groundwater hydrochemistry and quality assessment in hutuo river drinking water source area of Shijiazhuang (North China Plain). *Water (Switz.)* 16 (1). <https://doi.org/10.3390/w16010175>.
- Zhang, H., Cheng, S., Li, H., Fu, K., Xu, Y., 2020. Groundwater pollution source identification and apportionment using PMF and PCA-APCA-MLR receptor models in a typical mixed land-use area in Southwestern China. *Sci. Total Environ.* 741. <https://doi.org/10.1016/j.scitotenv.2020.140383>.
- Zhang, H., Han, X., Wang, G., Mao, H., Chen, X., Zhou, L., Huang, D., Zhang, F., Yan, X., 2023. Spatial distribution and driving factors of groundwater chemistry and pollution in an oil production region in the Northwest China. *Sci. Total Environ.* 875 (March), 162635. <https://doi.org/10.1016/j.scitotenv.2023.162635>.
- Zhang, Y., Xiao, Y., Yang, H., Wang, S., Wang, L., Qi, Z., Han, J., Hao, Q., Hu, W., Wang, J., 2024. Hydrogeochemical and isotopic insights into the genesis and mixing behaviors of geothermal water in a faults-controlled geothermal field on Tibetan Plateau. *J. Clean. Prod.* 442 (January), 140980. <https://doi.org/10.1016/j.jclepro.2024.140980>.
- Zhao, W., Qian, H., Xu, P., Yang, S., Liu, Y., Shen, Y., Zang, Y., Wang, Q., Cao, Z., 2024. Tracing groundwater-surface water sources and transformation processes in the Ba River Basin through dual isotopes and water chemistry. *Appl. Geochem.* 176 (October), 106199. <https://doi.org/10.1016/j.apgeochem.2024.106199>.
- Zhou, H., Yue, X., Chen, Y., Liu, Y., 2024. Source-specific probabilistic contamination risk and health risk assessment of soil heavy metals in a typical ancient mining area. *Sci. Total Environ.* 906 (947), 167772. <https://doi.org/10.1016/j.scitotenv.2023.167772>.